







ORIGINAL RESEARCH

Hepatic Abnormal Secretion of Apolipoprotein C3 Promotes Inflammation in Aortic Dissection

Xinghui Zhuang , MD^{*}; Mohammad Zarif, MD^{*}; Yue Shen, MD^{*}; Zhaofeng Zhang, MD; Jian He, MD; Linfeng Xie, MD; Qingsong Wu , MD; Xinfan Lin, MD; Keyuan Chen, MD; Yue Tian, MD; Yong Lin , MD; Yuling Zhang, MD; Ziwen Cai , MD, PhD; Zhihuang Qiu , MD, PhD; Liangwan Chen , MD, PhD

BACKGROUND: Apolipoprotein C3 (apo C3) is primarily secreted by the liver and is involved in promoting sterile inflammation and organ damage under pathological conditions. Previous studies have shown that apo C3 is abundant in the plasma exosomes of patients with aortic dissection (AD), but its specific role in AD remains unclear.

METHODS AND RESULTS: In vivo, adeno-associated virus was used to knock down hepatic apo C3 expression in an AD mouse model to assess the impact of liver-derived apo C3 on the development of AD. In vitro, recombinant apo C3 protein was added to the culture medium of J774A.1 macrophages to evaluate its effect on macrophage polarization and to identify the underlying mechanisms. Additionally, the effect of apo C3 on the function of aortic endothelial and smooth muscle cells was explored. Apo C3 in the aortas of AD mice was found to originate from abnormal hepatic secretion, which enters the bloodstream and subsequently deposits in the aorta. Adeno-associated virus-mediated hepatic apo C3 knockdown significantly reduced AD incidence ($P=0.0036$), macrophage infiltration ($P=0.0004$), and collagen deposition in the aorta ($P=0.0016$). Similarly, inhibiting the apo C3 receptor Toll-like receptor 2 significantly lowered AD incidence ($P=0.0352$). In vitro, recombinant apo C3 protein promoted M1 polarization and matrix metalloproteinase secretion in macrophages by activating the Toll-like receptor 2/NLR family pyrin domain containing 3 pathway. Additionally, apo C3 increased adhesion molecule expression in endothelial cells and induced inflammation, chemotaxis, and apoptosis in vascular smooth muscle cells.

CONCLUSIONS: Our findings highlight the role of abnormally secreted hepatic apo C3 in promoting aortic inflammation.

Key Words: aortic dissection ■ apolipoprotein C3 ■ inflammation ■ macrophages

Aortic dissection (AD) is a life-threatening condition with a high mortality rate, necessitating surgical intervention upon occurrence. If the ascending aorta experiences AD, 40% of patients face immediate death, with an hourly mortality rate of 1% to 2% and ~50% mortality rate within 48 hours.¹ Currently, there is a lack of pharmacological treatments for AD. Therefore, deciphering the pathogenesis of AD to

identify effective therapeutic targets is crucial. The pathophysiology of AD includes extracellular matrix degradation, smooth muscle cell phenotypic transition, oxidative stress, and inflammation.^{2–5} According to reports, innate immunity plays a crucial role in Stanford A-type acute AD. Macrophages are the primary immune cells infiltrating the aorta during acute AD onset, suggesting their potential major role in aortic

Correspondence to: Liangwan Chen, MD, PhD, Zhihuang Qiu, MD, PhD and Ziwen Cai, MD, PhD, Fujian Medical University, No. 29 Xinquan Road, Fuzhou 350001, China. Email: chenliangwan@fjmu.edu.cn; qzhflm@126.com; 171961014@qq.com

^{*}X. Zhuang, M. Zarif, and Y. Shen contributed equally.

Drs Chen, Qiu, and Cai, are now affiliated with the Engineering Research Center of Tissue and Organ Regeneration, Fujian Province University, Fuzhou, China. This manuscript was sent to Daniel T. Eitzman, MD, Senior Guest Editor, for review by expert referees, editorial decision, and final disposition.

Supplemental Material is available at <https://www.ahajournals.org/doi/suppl/10.1161/JAHA.124.037172>

For Sources of Funding and Disclosures, see page 23.

© 2025 The Author(s). Published on behalf of the American Heart Association, Inc., by Wiley. This is an open access article under the terms of the [Creative Commons Attribution-NonCommercial-NoDerivs](https://creativecommons.org/licenses/by-nc-nd/4.0/) License, which permits use and distribution in any medium, provided the original work is properly cited, the use is non-commercial and no modifications or adaptations are made.

JAHA is available at: www.ahajournals.org/journal/jaha

RESEARCH PERSPECTIVE

What Is New?

- This study demonstrates that abnormal deposition of apolipoprotein C3 (apo C3) in the aorta during aortic dissection is due to abnormal hepatic secretion into the bloodstream.
- Interfering with hepatic apo C3 can reduce aortic dissection incidence, macrophage infiltration, and extracellular matrix degradation in mice.
- Apo C3 in the aorta induces macrophage M1 polarization and matrix metalloproteinase release via the Toll-like receptor 2/NLR family pyrin domain containing 3 pathway, thereby promoting aortic inflammation and extracellular matrix degradation.

What Question Should Be Addressed Next?

- A large-scale prospective randomized controlled study is needed to further determine whether individuals with elevated apo C3 levels have an increased risk of aortic dissection.
- Explore the potential of apo C3 as a biomarker for predicting or early diagnosing aortic dissection.

Nonstandard Abbreviations and Acronyms

AAV	adeno-associated virus
apo C3	apolipoprotein C3
BAPN	β -aminopropionitrile
EC	endothelial cell
GO	gene ontology
INOS	inducible nitric oxide synthase
MAEC	mouse aortic endothelial cells
MMP	matrix metalloproteinase
MOVAS	mouse aortic vascular smooth muscle
NC	normal control
NLRP3	NLR family pyrin domain containing 3
TLR2	Toll-like receptor 2
WB	western blot
WT	wild-type

inflammation.⁶ In the ApoE^{-/-} Angiotensin II mouse model, continuous infusion of angiotensin II for 1 to 4 days results in macrophage infiltration into the aortic media, accompanied by elastic fiber degradation.⁷ In patients with acute AD, macrophages are distributed in the adventitial vessels and ruptured edges of the aorta,

where they secrete matrix metalloproteinases (MMPs), leading to degradation of the medial elastic fibers and subsequent medial degeneration.⁸ Although inflammation has been recognized during the development of AD, the specific mechanisms remain unclear, and the magnitude of its role in AD pathogenesis is yet to be determined. Particularly, the factors that activate immune cells to induce inflammation in the aorta during AD onset remain unanswered questions.

Previous studies have revealed a significant presence of apolipoprotein C3 (apo C3) in plasma exosomes from patients with AD compared with those from the control group, as indicated by plasma exosome sequencing. Apo C3 is primarily synthesized in the liver, with a minor fraction synthesized in the small intestine, suggesting a potential association between liver synthesis and the occurrence of AD.⁹ Physiologically, apo C3 plays a crucial role in the metabolism of triglyceride-rich lipoproteins. During the hydrolysis of very-low-density lipoprotein (VLDL) triglycerides mediated by lipoprotein lipase, apo C3 transfers from VLDL to high-density lipoprotein. Subsequently, apo C3 is transported back to the liver for the synthesis of new VLDL.¹⁰ Previous research indicates that apo C3 contributes to hypertriglyceridemia through various mechanisms.^{11–13} Under pathological conditions, compared with lipoproteins lacking apo C3, those containing apo C3, such as VLDL and low-density lipoprotein, increase monocyte adhesion to endothelial cells (ECs). Additionally, exposure of ECs to apo C3 or apo C3-enriched VLDL promotes the expression of vascular cell adhesion molecule 1 and intercellular adhesion molecule 1.¹⁴ Research has shown that apo C3 activates the NLR family pyrin domain containing 3 (NLRP3) inflammasome in human monocytes through Toll-like receptors 2 (TLR2) and 4.¹⁵ In renal diseases, apo C3 in the body inhibits EC regeneration and promotes renal damage through NLRP3-dependent activation of human monocytes.¹⁶

However, the role of apo C3 in AD has not been studied, and whether apo C3 acts as an endogenous pathogenic factor for AD remains unclear. Here, we identified the crucial role of apo C3 in the inflammation of AD. By suppressing liver apo C3 levels, we reduced aortic inflammation, thereby decreasing the occurrence of AD.

METHODS

The data that support the findings of this study are available from the corresponding author on reasonable request.

Study Design

This study aims to investigate the role of apo C3 in aortic dissection. We validated elevated apo C3 levels in

plasma, aortic tissues, and even liver tissues from patients with AD and mice to explore the primary source of apo C3 deposition in the arterial wall. In vivo experiments involved using adeno-associated virus (AAV) to knock down hepatic apo C3, assessing its impact on AD incidence and aortic inflammation. In vitro experiments focused on evaluating the effects of recombinant apo C3 protein on macrophage polarization and elucidating the underlying mechanisms. Additionally, we investigated apo C3's effects on EC adhesion and smooth muscle cell inflammation, chemotaxis, and apoptosis.

Collection of Human Specimens

Sample size calculation was performed using G*Power 3.1 with a statistical power of 0.80. Normal human aortic samples, blood, and clinical information were obtained from 40 heart transplant donors. Between January and March 2024, 40 consecutive patients with acute type A AD, who met the inclusion and exclusion criteria, were enrolled in the study. All patients underwent total arch replacement surgery at Fujian Medical University Union Hospital, during which aortic samples, blood, and clinical data were collected. All enrolled patients had a history of hypertension. Exclusion criteria included bicuspid aortic valve, Marfan syndrome, and other connective tissue disorders. Clinical characteristics of the enrolled subjects are presented in [Table S1](#). No significant differences were found between the 2 groups in terms of baseline characteristics ($P>0.05$).

The collection of human aortic specimens, blood samples, and clinical data was approved by the Ethics Review Committee of Fujian Medical University Union Hospital (Protocol No. 2023QH061) and conducted in accordance with the Declaration of Helsinki. Informed consent was obtained from all patients before surgery. Blood samples from patients with AD were collected immediately upon admission. Blood samples from both patients with AD and normal controls were centrifuged at 3000g for 15 minutes at 4 °C, and the supernatants were collected and stored at -80 °C until use.

To facilitate detailed analysis, we divided the samples into 2 groups: 20 pairs of AD patients and normal controls were used for plasma exosome sequencing, while the remaining 20 pairs were used for plasma ELISA validation.

Exosome Isolation and RNA Sequencing

Plasma samples were collected from patients with AD (n=20) and normal controls (n=20) at Fujian Medical University Union Hospital. The plasma was processed by sequential centrifugation: first at 300g for 15 minutes, then at 2000g for 15 minutes, and finally at 10000g for 30 minutes to obtain the supernatants. Exosomes were isolated from these supernatants

through ultracentrifugation at 120000g for 70 minutes. Total RNA was extracted from the isolated exosomes using TRIzol (Takara, Tokyo, Japan). The RNA samples were then sent to GMINIX Co., Ltd. (Shanghai, China) for RNA sequencing.

Mouse Study and AD Model

The mouse study protocol was approved by the Ethics Review Committee of Fujian Medical University (Protocol No. IACUC FJMU 2022-Y-0763). The sample size used was calculated using G*Power 3.1 software, which gave the statistical power of 0.80. Three-week-old C57BL/6J mice were purchased from GemPharmatech Co., Ltd. Throughout the animal experiment, mice had free access to ample pellet food and water. For the AD model, 4-week-old male mice were fed a normal diet and administered freshly prepared β -aminopropionitrile (BAPN; TCI) solution dissolved in the drinking water (0.25%) for 4 weeks. Two days before euthanasia, angiotensin II (1.44 mg/kg per day; Glpbio) was administered via intraperitoneal injection.

For the hepatic apo C3 interference model, mice were assigned to 4 groups: wild-type (WT), BAPN, BAPN+Sh-apo C3, and BAPN+Sh-normal control (NC). BAPN+Sh-apo C3 and BAPN+Sh-NC groups were injected with AAV-Sh-apo C3 and AAV-Sh-NC via the angular vein at 3 weeks of age. For the TLR2 inhibitor C29 model, mice were divided into WT, BAPN, and BAPN+C29 groups. The BAPN+C29 group received 25 mg/kg C29 (MCE) via gavage every other day from 4 to 8 weeks of age. All groups, except WT, were fed 0.25% BAPN for 4 weeks and injected with angiotensin II for the last 2 days.

Criteria for Dissection

AD is a condition in which a tear in the intimal layer and disruption of the medial layer of the aortic wall, caused by a combination of wall stress and abnormalities, allows blood to penetrate and separate the layers of the aortic wall. During the experimental process, deceased mice exhibited blood clots filling the thoracic cavity, with the clots completely enveloping the heart, indicating the occurrence and rupture of AD. The aortas were excised and fixed in 4% paraformaldehyde for 48 hours. For the remaining mice, which had undergone 28 days of modeling, the aortas were similarly fixed in 4% paraformaldehyde for 48 hours after anesthesia. The tissues were embedded in paraffin, sectioned into 4- μ m-thick slices, and stained with hematoxylin and eosin. Morphological changes in the vascular walls were observed under an optical microscope. The presence of a significant false lumen formation was used to determine the occurrence of AD. The incidence of AD=Number of mice with AD/Total number of mice.

Construction of Virus-Infected Mice and In Vivo Imaging

A recombinant AAV containing the mouse apo C3 gene was purchased from Hanheng Biotechnology Co., Ltd. (Shanghai, China). The AAV, HBAAV2/8-m-apo C3 shRNA-LUC (1.2×10^{12} viral genomes/ μ L), was constructed and synthesized by HANBIO (Shanghai, China). Three-week-old mice were injected with 10^{11} vg of AAV serotype 2/8 (Hanbio Biotechnology, Shanghai, China): AAV-NC and AAV-Sh-apo C3, diluted in 100 μ L PBS, respectively, via the angular vein. The AAV eventually infects the liver through the venous system. Small interfering RNA (siRNA) targets were designed on the basis of apo C3 transcripts, and primers were synthesized accordingly. The single-stranded primers were annealed into double-stranded oligo sequences and ligated into a double-enzyme linearized RNA interference vector (Hanbio Biotechnology). The sequences used were apo C3-siRNA (GGAGCAAGTTTACTGACAA) and NC-siRNA (TTCTCCGAACGTGTCACGTAA). The selected oligos were then cloned into the linearized pHBAAV-U6-MCS-CMV-EGFP vector (Hanbio Biotechnology) using T4 DNA ligase.

For in vivo imaging, due to the presence of a luciferase-encoding gene (*Luc*) in the plasmid vector, 7-week-old mice were intraperitoneally injected with D-luciferin potassium salt (Yeasen). Bioluminescence imaging was then used to detect the location and intensity of fluorescence.

Lipid Measurement Methods

For lipid profile analysis, blood samples were collected and stored at 4 °C overnight. After storage, the samples were centrifuged at 3000 rpm for 15 minutes at 4 °C, and the supernatant was immediately analyzed. Lipid measurements were performed using an automated biochemical analyzer (Wuhan Servicebio Technology Co., Ltd) to determine triglycerides, total cholesterol, high-density lipoprotein cholesterol, and low-density lipoprotein cholesterol.

Measurement of Aortic Diameter

The maximum aortic diameter in the representative images of each group of mice was measured using ImageJ version 1.8.0 software, based on the scale bar.

Cell Culture

Mouse aortic vascular smooth muscle (MOVAS; BeNa Culture Collection; BNCC338213) cells, mouse aortic ECs (MAECs; BeNa Culture Collection; BNCC359881), and J774A.1 cells (Procell; CL-0370) were cultured in high-glucose medium (Procell; PM150210) containing 10% FBS (HAKATA). The cells were maintained

in a humidified incubator at 37 °C with 5% CO₂. Recombinant Mouse Apolipoprotein C3 (CUSABIO; CSB-EP001933MO) was added to MOVAS, MAECs, and J774A.1 cells at different concentrations and incubated for 48 hours.

Western Blotting and Coimmunoprecipitation

Human aortic tissue, mouse aorta, and J774A.1 cells were lysed in RIPA buffer to extract total proteins. Protein concentration was determined using the BCA Protein Quantification Kit (Yeasen). Equal amounts of total protein were loaded onto 12% SDS-PAGE gels (GenScript) and transferred to 0.22 μ m PVDF membranes (Immobilon). The membranes were blocked with 5% nonfat milk at room temperature for 2 hours and then incubated overnight at 4 °C with primary antibodies against apo C3 (1:1000; Affinity; DF8054), TLR2 (1:1000; Proteintech; 17236-1-AP), NLRP3 (1:1000; Invitrogen; MA5-23919), cluster of differentiation 86 (CD86) (1:1000; Proteintech; 13395-1-AP), inducible nitric oxide synthase (iNOS) (1:1000; Invitrogen; PA1-036), matrix metalloproteinase (MMP) 2 (1:1000; Proteintech; 10373-2-AP), and MMP9 (1:1000; Proteintech; 10375-2-AP). The next day, the membranes were incubated at room temperature for 2 hours with HRP-conjugated secondary antibodies (Beyotime). Specific immunoreactive protein bands were detected using the Super ECL Detection Reagent (Yeasen) and analyzed with ImageJ.

In the coimmunoprecipitation experiment, J774A.1 macrophages were treated with 50 μ g/mL apo C3 for 48 hours before total protein extraction. Immunoprecipitation was performed using the apo C3 antibody to obtain a protein complex, and the presence of TLR2 protein in the complex was validated by western blot (WB). Conversely, after immunoprecipitation with the *Tlr2* antibody, the presence of apo C3 protein in the complex was also confirmed by WB.

RNA Extraction and Polymerase Chain Reaction

Total RNA was isolated using RNAiso Plus reagent (Takara; 9109). The total RNA was reverse transcribed into cDNA using the PrimeScript RT reagent Kit (Perfect Real Time; Takara; RR037A). TB Green Premix Ex Taq II (Tli RNaseH Plus; Takara; RR820A) was used according to the manufacturer's instructions. The polymerase chain reaction (PCR) program included an initial denaturation step at 95 °C for 30 seconds, followed by 40 cycles of denaturation at 95 °C for 5 seconds and annealing/extension at 60 °C for 30 seconds. Primers for target genes were synthesized by SunYa Company (Zhejiang, China). The primer sequences (5' to 3') are as follows:

Apo C3: F: TCAGCTTCATGCAGGGTTACA, R: CCT TAACGGTGCTCCAGTAGT

Apoc3: F: GGCTGGATGGACAATCACTTC, R: TTG GTTGGTCCTCAGGGTTAG

Cd86: F: TGCACGTCTAAGCAAGGTCA, R: CCAGA ACACACACAACGGTC

Inos: F: GGAGTGACGGCAAACATGACT, R: TCGAT GCACAACCTGGGTGAAC

Tlr2: F: TTCACCACTGCCCCTAGATG, R: CGCTCAC TACGTCTGACTCC

Nlrp3: F: TCCCAGACACTCATGTTGCC, R: GTCCAG TTCAGTGAGGCTCC

Cxcl1: F: CGCCTATCGCCAATGAGCTG, R: GACTT CGGTTTGGGTGCAGT

Cxcl5: F: CCCTTCCTCAGTCATAGCCG, R: CTTCCA CCGTAGGGCACTG

Ccl2: F: CACCTGCTGCTACTCATTCAC, R: TGTCTG GACCCATTCTTCTT

Ccl7: F: GCTGCTTTTCAGCATCCAAGT, R: ACCCAC TTCTGATGGGCTTC

Saa3: F: AGAGAGGCTGTTTCAAGATTCA, R: AGC AGGTCGGAAGTGTTG

Il-6: F: CTGCAAGAGACTTCCATCCAG, R: AGTGG TATAGACAGGTCTGTTGG

a-sma: F: GCATCCACGAAACCACCTATAAC, R: AC AGAGTACTTGCGTTCTGGAG

Opn: F: AGCAAGAACTCTTCCAAGCAA, R: GTGA GATTTCGTCAGATTCATCCG

Pecam-1: F: CTGGTACCGATCCAGGTGTG, R: GTT GCTGGGTCATTGGAGGT

Vcam-1: F: CTGTGACAATGACCTGTTCCA, R: AGA GTCTTCCATCCTCATAGCA

Icam-1: F: TCCGTGGGGAGGAGATACTG, R: TGAG ATCCAGTTCTGTGCGG

E-selectin: F: GCTACCCATGGAACACGACA, R: CT TTGCATGATGGCGTCTCG

Gapdh: F: TGGAAAGCTGTGGCGTGATG, R: TACTT GGCAGGTTTCTCCAGG

GAPDH: F: GGTGTGAACCATGAGAAGTATGA, R: GAGTCCTTCCACGATACCAAAG

Immunohistochemistry

Human and mouse aortas were dehydrated, embedded, and sectioned to prepare paraffin sections. After deparaffinization and antigen retrieval, immunohistochemical staining was performed using the UltraSensitive SP (mouse/rabbit) IHC Kit (MXB; KIT-9710). The sections were incubated overnight at 4 °C with primary antibodies against apo C3 (1:200; DF8054, Affinity), TLR2 (1:200; Proteintech; 17236-1-AP), NLRP3 (1:200; Invitrogen; MA5-23919), CD86 (1:200; Proteintech; 13395-1-AP), INOS (1:200; Invitrogen; PA1-036), MMP2 (1:200; 10373-2-AP, Proteintech), and MMP9 (1:200; Proteintech; 10375-2-AP). Finally, the sections were stained with 3,3'-diaminobenzidine

for the same duration. Protein expression levels were evaluated using ImageJ with the same analysis settings parameters to determine the average density of protein expression in each image.

Immunofluorescence

For tissue immunofluorescence, paraffin blocks containing aortic tissues were obtained, and 5- μ m sections were prepared. After deparaffinization, antigen retrieval was performed. For cell immunofluorescence, cells were fixed with 4% paraformaldehyde and washed with PBS 3 times. Then, permeabilization was carried out with 0.2% Triton X-100 for 20 minutes, followed by blocking with 5% BSA for 1 hour. Primary antibodies against apo C3 (1:100; Affinity; DF8054), TLR2 (1:100; Proteintech; 17236-1-AP), NLRP3 (1:100; Invitrogen; MA5-23919), CD86 (1:100; Proteintech; 13395-1-AP), INOS (1:100; Invitrogen; PA1-036), MMP2 (1:100; Proteintech; 10373-2-AP), MMP9 (1:100; Proteintech; 10375-2-AP), CD68 (1:100; Invitrogen; 14-0688-82), F4/80 (1:100; Invitrogen; 14-4801-82), CD31 (1:100; Abcam; ab9498) and α -smooth muscle actin (1:100; Boster; BM4172), were incubated overnight at 4 °C. The next day, corresponding species-specific fluorescence secondary antibodies (Alexa Fluor 488 and tetramethylrhodamine) were incubated for 2 hours at room temperature. Then, DAPI solution (Solarbio; C0065) was added to stain the nuclei for 10 minutes. Finally, mounting medium with antifade reagent (Yeast; 36307ES08) was added to seal the slides. Immunofluorescence images were captured using a fluorescence microscope, and ImageJ was used to evaluate the average fluorescence intensity of protein expression in each image under the same analysis settings parameters.

Enzyme-Linked Immunosorbent Assay

We used the Human Apolipoprotein C3 ELISA Kit (Mei Ke; MK4381A) and the Mouse Apolipoprotein C3 ELISA Kit (Mei Ke; MK6122A) to measure the expression levels of apo C3 in human and mouse plasma, respectively.

Flow Cytometry

To analyze the M1 polarization of J774A.1 cells after apo C3 intervention by flow cytometry, J774A.1 cells from the apo C3 group and the saline group were pelleted and washed to remove the culture medium. After incubating with corresponding antibodies at 4 °C for 30 minutes, the cells were transferred to flow cytometry tubes and analyzed using the LSR FortessaX-20 Cell Analyzer (BD Bioscience). M1 population was identified by F4/80⁺CD86⁺ gating. Antibodies used were PE Rat Anti-Mouse F4/80 (BD Bioscience; 565410) and APC Rat Anti-Mouse CD86 (BD Bioscience; 558703).

Mouse Aorta Histological Staining

Mouse aortic paraffin blocks were sectioned into 4- μ m slices and deparaffinized and dehydrated. For hematoxylin and eosin staining, the sections were stained with hematoxylin for 5 minutes, followed by 30 seconds of differentiation in 1% hydrochloric acid ethanol to remove excess hematoxylin. After staining with 0.5% eosin for 3 minutes, the sections were rinsed with running water and dehydrated before mounting. Masson's staining (Solarbio Life Science; G1340) and Elastic Van Gieson staining (Genye Biotechnology; R203913) were performed according to the manufacturer's instructions. Finally, changes in elastic fibers and collagen fibers were analyzed using a Nikon fluorescence microscope (Nikon ECLIPSE Ni, Japan) and ImageJ.

RNA Sequencing and Analysis

Total RNA from mouse aorta and MOVAS was isolated using RNAiso Plus (Takara; 9109). RNA sequencing was performed by LC-Bio Inc. (Hangzhou, China). Differentially expressed mRNAs were selected with fold change >2 or fold change <0.5 and P value <0.05 using the R package edgeR (<http://www.r-project.org/>). Subsequently, the differentially expressed mRNAs were subjected to gene ontology (GO) enrichment and Kyoto Encyclopedia of Genes and Genomes pathway analysis. Volcano plots, heat maps, GO, and Kyoto Encyclopedia of Genes and Genomes analyses were performed using the OmicStudio tools at <https://www.omicstudio.cn>. As the P values for the volcano plots were calculated using the Wald test in DESeq2, the false discovery rate was automatically controlled using the Benjamini–Hochberg method. The protein–protein interaction networks among the differentially expressed genes were analyzed using the STRING database (<https://www.string-db.org/>).

Cell Proliferation and Migration-Level Detection

For the scratch assay, MOVAS cells were incubated with apo C3 for 48 hours and seeded in 6-well cell culture plates at a density of 5×10^6 cells/well alongside control group cells. After removing the culture medium, a 200 μ L pipette tip was used to create a scratch, followed by washing with PBS to remove floating cells, and fresh culture medium was added. The wound healing process was recorded and measured at 0 and 24 hours. The migration area was calculated using ImageJ software by subtracting the healed wound area from the original wound area. For the Cell-Counting Kit-8 assay, cells were seeded at a density of 2000 cells/well in a 96-well plate. Cell proliferation levels were detected at 0, 24 and 48 hours using the Cell-Counting Kit-8 (YEASEN;

40203ES76). For the 5-ethynyl-2'-deoxyuridine assay, cells were seeded at a density of 5×10^6 cells/well in a 6-well plate. Cell proliferation levels were detected at 24 hours using the 5-ethynyl-2'-deoxyuridine assay kit (BeyoClick, EdU Cell Proliferation Kit with Alexa Fluor 488; Beyotime; C0071L).

Cell Apoptosis-Level Detection

To detect changes in apoptosis levels after apo C3 intervention in MOVAS cells, cells were seeded at a density of 5×10^6 cells/well in a 6-well plate. Apoptosis levels were detected at 24 hours using the apoptosis assay kit (One Step TUNEL Apoptosis Assay Kit; Beyotime; C1088).

Macrophage Adhesion Experiment

Endothelial cells were divided into 4 groups: saline 1-minute group, saline 5-minute group, apo C3 1-minute group, and apo C3 5-minute group. The saline 1-minute group and saline 5-minutes group were untreated ECs, to which suspended J774A.1 cells were added for 1 minute and 5 minutes, respectively. The apo C3 1-minute group and apo C3 5-minute group were ECs pretreated with apo C3 for 48 hours, to which suspended J774A.1 cells were added for 1 minute and 5 minutes, respectively. Subsequently, macrophages adhered to the ECs, and immunofluorescence staining was performed. The number of macrophages adhered to ECs divided by the total number of cells reflects the EC adhesion capability.

Statistical Analysis

Categorical data are given as proportions, and continuous variables are expressed as mean \pm SD. The baseline characteristics table was created using the gtsummary package in R version 4.1.3 (R Foundation for Statistical Computing, Vienna, Austria). Univariate and multivariable logistic regression analyses were conducted using SPSS Statistics version 29.0 (IBM, Armonk, NY) to calculate odds ratios (ORs) and 95% CIs. Restricted cubic spline curves were plotted using the plotRCS function from the rms R package to examine the relationship between plasma apo C3 levels and the occurrence of aortic dissection, illustrating the OR for each unit increase in apo C3. Based on the results of the restricted cubic spline curve, plasma apo C3 levels were categorized into low and high groups using the apo C3 value corresponding to an OR of 1. Age, sex, body mass index, smoking, and alcohol consumption were included as covariates in the analysis to assess the relationship between apo C3 levels and aortic dissection.

Results from multiple observations are presented as mean \pm SEM. Experiments were typically conducted

independently at least 3 times to ensure data reproducibility. All graphs and calculations were performed using Prism 8.0.1 (GraphPad Software, San Diego, CA). Normality was tested using the Shapiro–Wilk test. If the data followed a normal distribution, we applied the unpaired *t* test for 2-group comparisons and 1-way ANOVA for comparisons among multiple groups, assuming equal variances. If the data did not follow a normal distribution, we used the Mann–Whitney *U* test for 2-group comparisons and the Kruskal–Wallis test for comparisons among multiple groups. For the Kruskal–Wallis test, *P* values were adjusted using Dunn’s multiple comparisons test, and for the 1-way ANOVA, we used Tukey’s multiple comparisons test. The dose–effect-related data were analyzed using the Kruskal–Wallis test to assess group differences and the Jonckheere–Terpstra test to evaluate the monotonic trend across different dose levels. A bar graph was chosen to clearly display the differences between

groups and facilitate comparison. The data points on the bar graph represent the actual values for each biological sample, and the presented data points include all the original data. The incidence of AD across different groups was assessed with the χ^2 test, while the survival curves were evaluated using the log-rank test. Values were considered significant at *P*<0.05.

RESULTS

Apo C3 Abundantly Present in Plasma of Patients With AD and Deposits in the Aorta

Previous sequencing of plasma exosomes from 20 AD patients and 20 NCs revealed a significant presence of apo C3 in the plasma exosomes of patients with AD (Figure 1A). We also validated the changes in apo C3 levels in the plasma of another cohort of 20

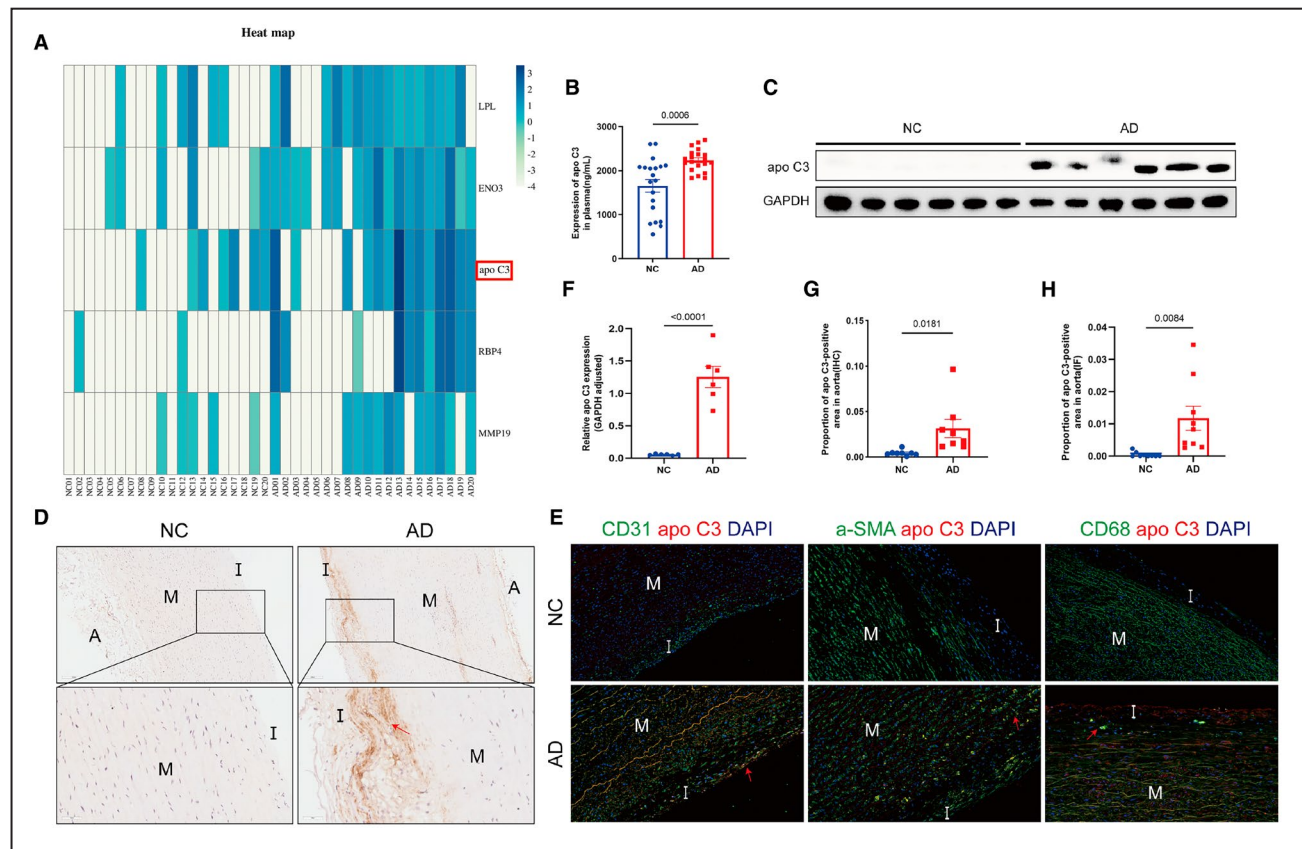


Figure 1. Apo C3 is abundant in the plasma of patients with AD and deposits in the aorta.

A, Heat map results of plasma exosome sequencing in patients with AD (*n*=20) and normal controls (*n*=20). **B**, ELISA results of apo C3 in the plasma of patients with AD (*n*=20) and NCs (*n*=20). **C**, Representative western blot of apo C3 protein in the aortas of patients with AD (*n*=6) and NCs (*n*=6). **D**, Representative immunohistochemistry of apo C3 in the aortas of patients with AD (*n*=8) and normal controls (*n*=8). **E**, Representative immunofluorescence of apo C3 in the aortas of patients with AD (*n*=9) and normal controls (*n*=9). **F** through **H**, Quantitative protein levels of apo C3 in western blot (**C**), immunohistochemistry (**D**), and immunofluorescence (**E**). Data are expressed as mean±SEM. Bars represent the means, and caps represent the SEM. Statistical comparisons were made using an unpaired *t* test (**B**, **F** through **H**). A value of *P*<0.05 was considered significant. The layers of the aorta are denoted as I for intima, M for media, and A for adventitia. AD indicates aortic dissection; apo C3 apolipoprotein C3; α-SMA, α-smooth muscle actin; CD: cluster of differentiation; ENO, enolase; LPL, lipoprotein lipase; MMP, matrix metalloproteinase; NC, normal control; and RBP, retinol-binding protein.

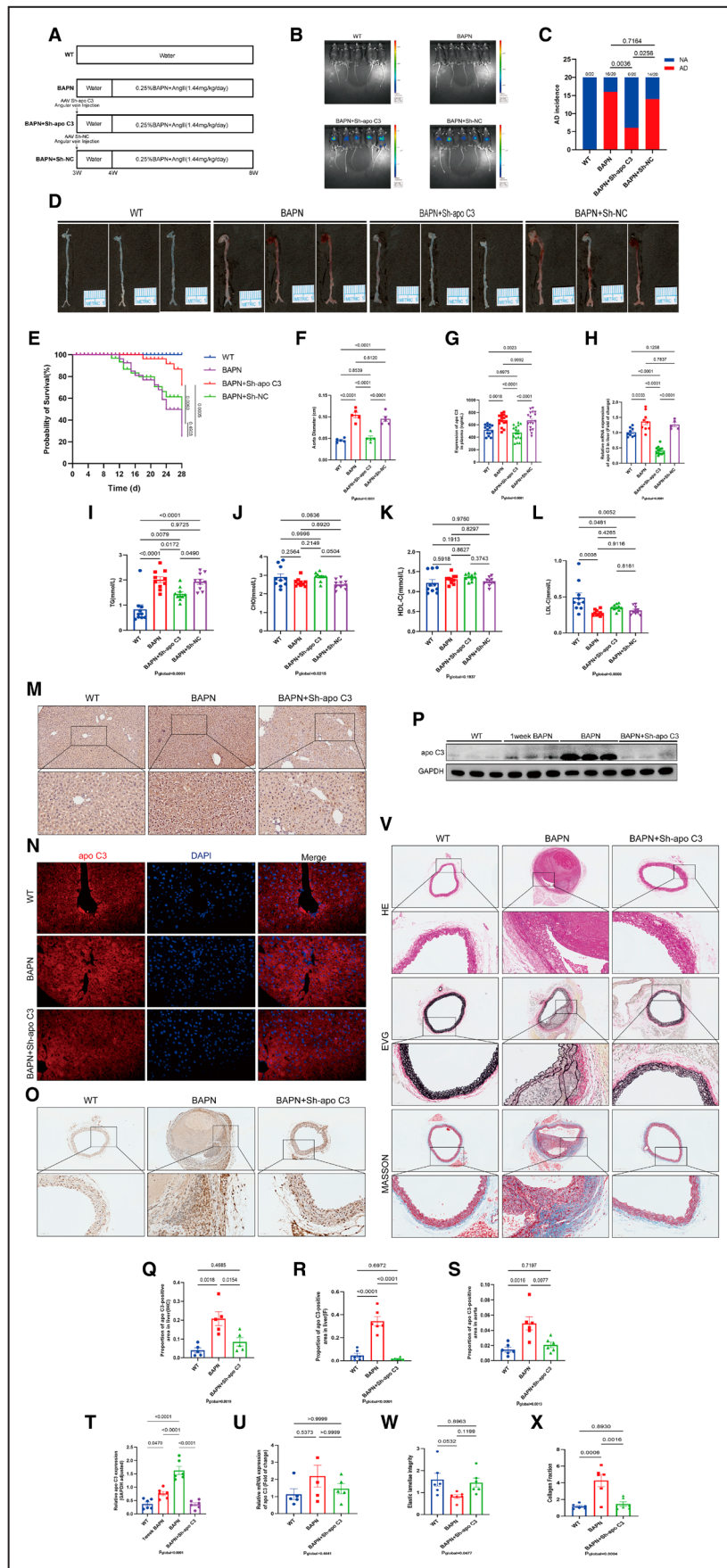
patients with AD and 20 normal controls. The results confirmed a widespread increase in apo C3 levels in the plasma of patients with AD (Figure 1B). As shown in the baseline characteristics table, there were no statistically significant differences in age, sex, body mass index, and other data between the patients with AD and NCs included in this study (Table S1). The univariate logistic regression analysis for apo C3 revealed an OR of 9.00 (95% CI, 2.31–41.75; $P=0.003$). Based on the results of the restricted cubic spline curve, plasma apo C3 levels were categorized into low and high groups using the apo C3 value corresponding to an OR of 1 (2088.551 ng/mL) (Figure S1). After adjusting for age, sex, body mass index, smoking, and alcohol consumption, the adjusted OR was 11.28 (95% CI, 2.55–66.34; $P=0.003$). These results suggest that apo C3 is a risk factor for aortic dissection, independent of the factors mentioned above (Table S2). WB analysis showed high expression of apo C3 in the aortas of patients with AD (Figure 1C and 1F). The immunohistochemistry and immunofluorescence staining both showed apo C3 deposition in the endothelial layer and sub-endothelial layer of the aorta, and even on the intimal side of the medial layer. Furthermore, apo C3 exhibited notable colocalization with endothelial cells, smooth muscle cells, and macrophages (Figure 1D and E and 1G and H). We assessed apo C3 mRNA levels in human aortic tissue using PCR and found almost no detectable apo C3 mRNA, suggesting that the apo C3 deposited in the aorta is not produced by the aorta itself. These findings indicate that although apo C3 is abundantly present in the plasma and aortic tissue of patients with AD, it seems to be not synthesized by the aorta.

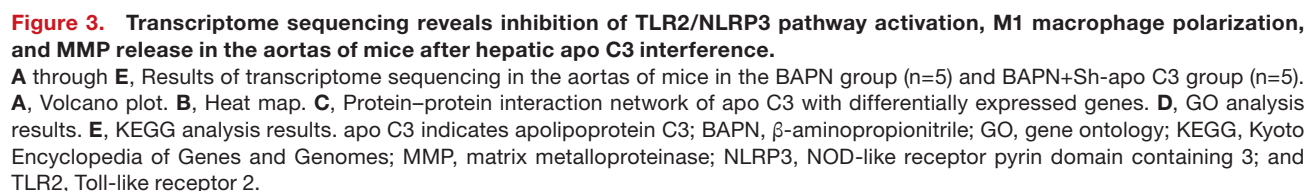
Hepatic Oversecretion of Apo C3 Leads to Apo C3 Deposition in the Aorta, Promoting Mouse AD Occurrence and Extracellular Matrix Degradation

Details of the animal groups are provided in Figure 2A. Due to the AAV-ShRNA carrying the luciferase gene, in vivo imaging showed that both AAV viruses had infected the liver (Figure 2B). The final animal results showed that the incidence of AD in the BAPN+Sh-apo C3 group (6/20) was significantly lower than in the BAPN group (16/20) ($P=0.0036$) and the BAPN+Sh-NC group (14/20) ($P=0.0256$), while there was no significant difference in incidence between the BAPN group and the BAPN+Sh-NC group ($P=0.7164$) (Figure 2C). Figure 2D shows representative images of aortas from each group. The survival curve results in Figure 2E show that the survival rate of mice in the BAPN+Sh-apo C3 group was higher at 28 days compared with the BAPN group ($P=0.0005$) and the BAPN+Sh-NC group ($P=0.0063$). This suggests that interference with hepatic apo C3 can reduce AD deaths. Figure 2F shows the differences in maximum aortic diameter among the groups of mice. The results indicate that the maximum aortic diameter in the BAPN+Sh-apo C3 group was significantly smaller than that in the BAPN group ($P<0.0001$) and the BAPN+Sh-NC group ($P<0.0001$), but there was no significant difference compared with the WT group ($P=0.8539$). This suggests that interfering with liver apo C3 can reduce aortic dilation induced by AD modeling. Lipid profile analysis shows that AD mice exhibited elevated triglyceride levels ($P<0.0001$) and reduced low-density lipoprotein cholesterol levels ($P=0.0008$), while cholesterol ($P=0.2564$) and high-density lipoprotein

Figure 2. Excessive hepatic secretion of apo C3 leads to its deposition in the aorta, promoting AD occurrence and extracellular matrix degradation.

A, Schematic diagram of AD mouse modeling process. **B**, Representative live imaging pictures of mice. **C**, AD incidence rates in each group ($n=20$ per group). **D**, Representative photographs of the aorta from each group of mice. **E**, Survival curves of mice in each group. **F**, The aortic diameter of each group of mice ($n=5$ per group). **G**, ELISA results for apo C3 levels in plasma were obtained from the following mouse groups: WT ($n=14$), BAPN ($n=16$), BAPN+Sh-apo C3 ($n=17$), and BAPN+Sh-NC ($n=17$). **H**, Hepatic apo C3 mRNA levels were measured in the following mouse groups: WT ($n=9$), BAPN ($n=9$), BAPN+Sh-apo C3 ($n=12$), and BAPN+Sh-NC ($n=5$). **I** through **L**, The levels of triglycerides, cholesterol, HDL-C, and LDL-C in the blood of mice in each group ($n=10$ per group). **M**, Representative immunohistochemistry of apo C3 in the liver of mice ($n=5$ per group). **N**, Representative immunofluorescence of apo C3 in the liver of mice ($n=6$ per group). **O**, Representative immunohistochemistry of apo C3 in the aortas of mice ($n=6$ per group). **P**, Representative western blot of apo C3 in the aortas of mice ($n=6$ per group). **Q**, Quantification of apo C3 protein levels in liver immunohistochemistry (**M**). **R**, Quantification of apo C3 protein levels in liver immunofluorescence (**N**). **S**, Quantification of apo C3 protein levels in aorta immunohistochemistry (**O**). **T**, Quantification of apo C3 protein levels in aorta western blot (**P**). **U**, Apo C3 mRNA levels in the aortas of mice in each group ($n=5$ per group). **V**, Representative images of HE staining, EVG staining, and Masson staining of the aortas of mice ($n=6$ per group). **W** through **X**, Quantification of elastic fiber and collagen fiber areas in aorta histological staining (**V**). The data are expressed as mean \pm SEM. Bars represent the means, and caps represent the SEM. Comparisons of AD incidence were analyzed using Fisher's exact test (**C**). Comparisons of survival curves were analyzed using the log-rank test (**E**). Statistical significance was determined by Kruskal–Wallis test with Dunn's multiple comparison test in **U**, and determined by 1-way ANOVA with Tukey's multiple comparisons test in **F** through **L**, **Q** through **T**, and **W** through **X**. A value of $P<0.05$ was considered significant. AD indicates aortic dissection; apo C3, apolipoprotein C3; BAPN, β -aminopropionitrile; CHO, cholesterol; EVG, Elastic Van Gieson; HDL-C, high-density lipoprotein cholesterol; HE, hematoxylin and eosin; LDL-C, low-density lipoprotein cholesterol; NC, normal control; TG, triglycerides; and WT, wild-type.





C3 group (Figure 2H). Immunohistochemistry and immunofluorescence staining of mouse liver tissues showed that apo C3 protein levels were higher in the BAPN group than in the WT group, and lower in the BAPN+Sh-apo C3 group (Figure 2 M-N and 2Q-R). These results indicate that AAV-Sh-apo C3 successfully interfered with the expression of Apoc3 mRNA and protein levels in the liver. Interference with hepatic apo C3 also resulted in reduced plasma apo C3 levels, suggesting that apo C3 produced by the liver is released into the bloodstream. Importantly, when AD occurs, the liver secretes large amounts of apo C3 into the blood, and interference with hepatic apo C3 reduces the incidence of AD, indicating that hepatic secretion of apo C3 promotes the occurrence of AD. Immunohistochemistry results of mouse aortas showed that apo C3 was abundantly deposited in the endothelial and subendothelial layers of the aorta in the BAPN group, and deposition

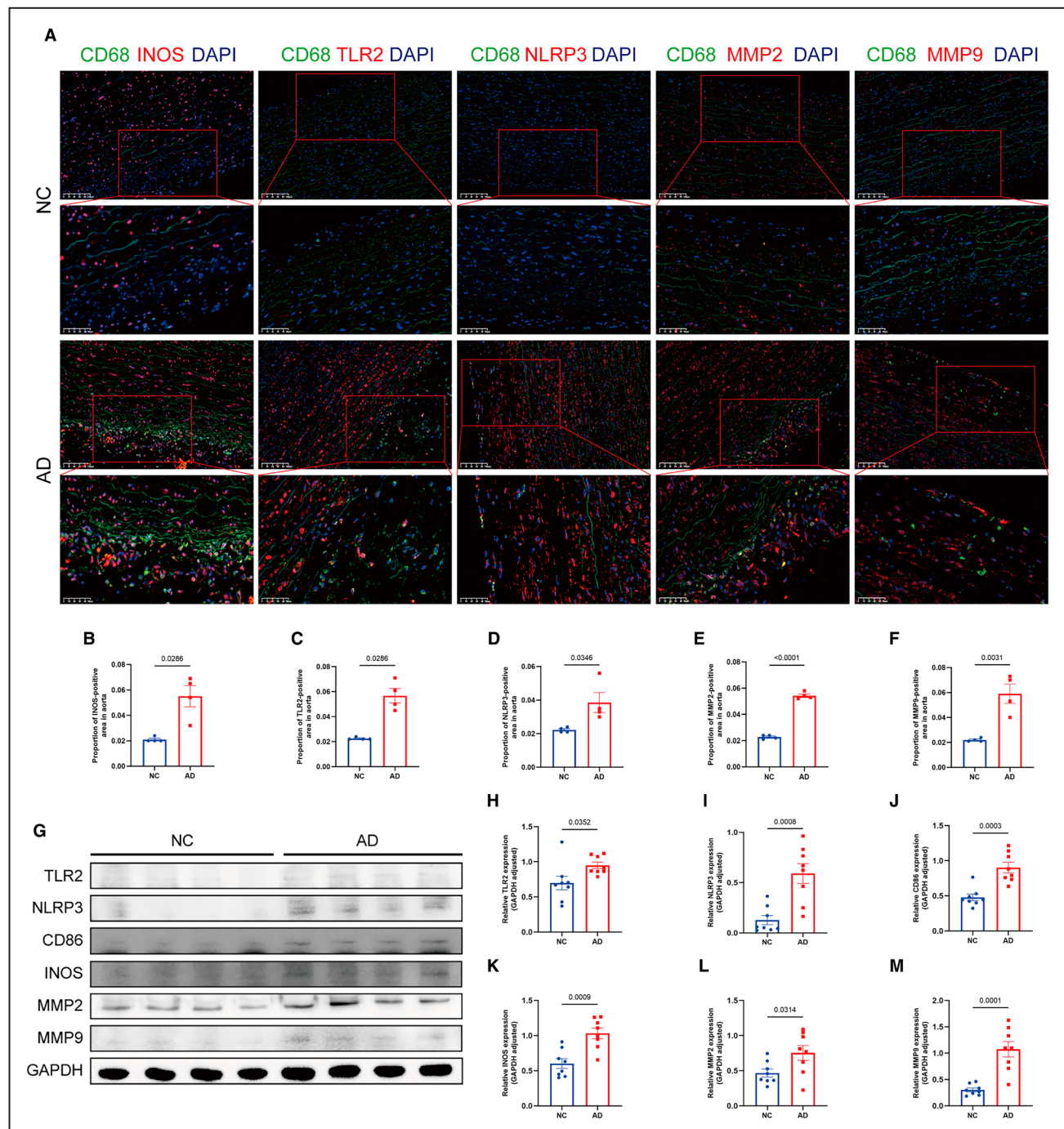


Figure 4. The aortas of patients with AD exhibit abundant M1 macrophages, with significant activation of the TLR2/NLRP3 signaling pathway, and increased release of MMP2 and MMP9.

Representative immunofluorescence (A) of aortas from patients with AD (n=4) and normal controls (n=4), with quantification of INOS (B), TLR2 (C), NLRP3 (D), MMP2 (E), and MMP9 (F) expression in patients with AD and normal controls. Representative western blot (G) of aortas from patients with AD (n=8) and normal controls (n=8), with quantification of TLR2 (H), NLRP3 (I), CD86 (J), INOS (K), MMP2 (L), and MMP9 (M) expression in patients with AD and normal controls. Data are presented as mean±SEM. Bars represent the means, and caps represent the SEM. Statistical significance was determined by Mann–Whitney U test in (B) and (C) and by unpaired t test in D through F and H through M. A value of $P < 0.05$ was considered significant. AD indicates aortic dissection; CD, cluster of differentiation; INOS, inducible nitric oxide synthase; MMP, matrix metalloproteinase; NLRP3, NOD-like receptor pyrin domain containing 3; and TLR2, Toll-like receptor 2.

decreased after interference with hepatic apo C3 expression (Figure 2O and 2S). The WB results show that, compared with the WT group, the protein level of apo C3 in the aorta was already increased after 1 week of BAPN treatment ($P=0.0470$), and this expression significantly increased over time, reaching a higher level at 4 weeks ($P<0.0001$). Additionally, suppression of hepatic apo C3 led to a significant reduction in aortic apo C3 expression ($P<0.0001$) (Figure 2P and 2T). To investigate the source of apo C3 in mouse aortas, PCR results showed no statistically significant difference in apo C3 mRNA levels in mouse aortas (Figure 2U). Therefore, the deposition of apo C3 in mouse aortas is caused by liver abnormal release into the blood during the occurrence of AD. The histological staining results of mouse aortas in Figure 2V showed that, compared with the BAPN group, the BAPN+Sh-apo C3 group exhibited a more intact aortic structure, with reduced elastic fiber fragmentation ($P=0.1199$, although not statistically significant) and decreased collagen deposition ($P=0.0016$) (Figure 2W through 2X). This indicates that interference with hepatic apo C3 significantly improves extracellular matrix degradation.

Transcriptome Sequencing Revealed That Interference With Apo C3 in the Liver Inhibited the Activation of the TLR2/NLRP3 Pathway, M1 Macrophage Polarization, and MMP Release in Mouse Aortas

Transcriptome sequencing was conducted on the aortas of mice from the BAPN group and the BAPN+Sh-apo C3 group. The volcano plot showed 510 upregulated genes and 155 downregulated genes among differentially expressed genes (Figure 3A). The heat map demonstrated that the levels of M1 macrophage markers (*Cd80*, *Cd86*), inflammatory factors (*TNF- β* , *Il-1 β* , *Il-6*, *Il-18*), and MMPs (*Mmp2*, *Mmp9*) were downregulated in the BAPN+Sh-apo C3 group (Figure 3B). GO analysis indicated that processes such as arterial inflammation, positive regulation of

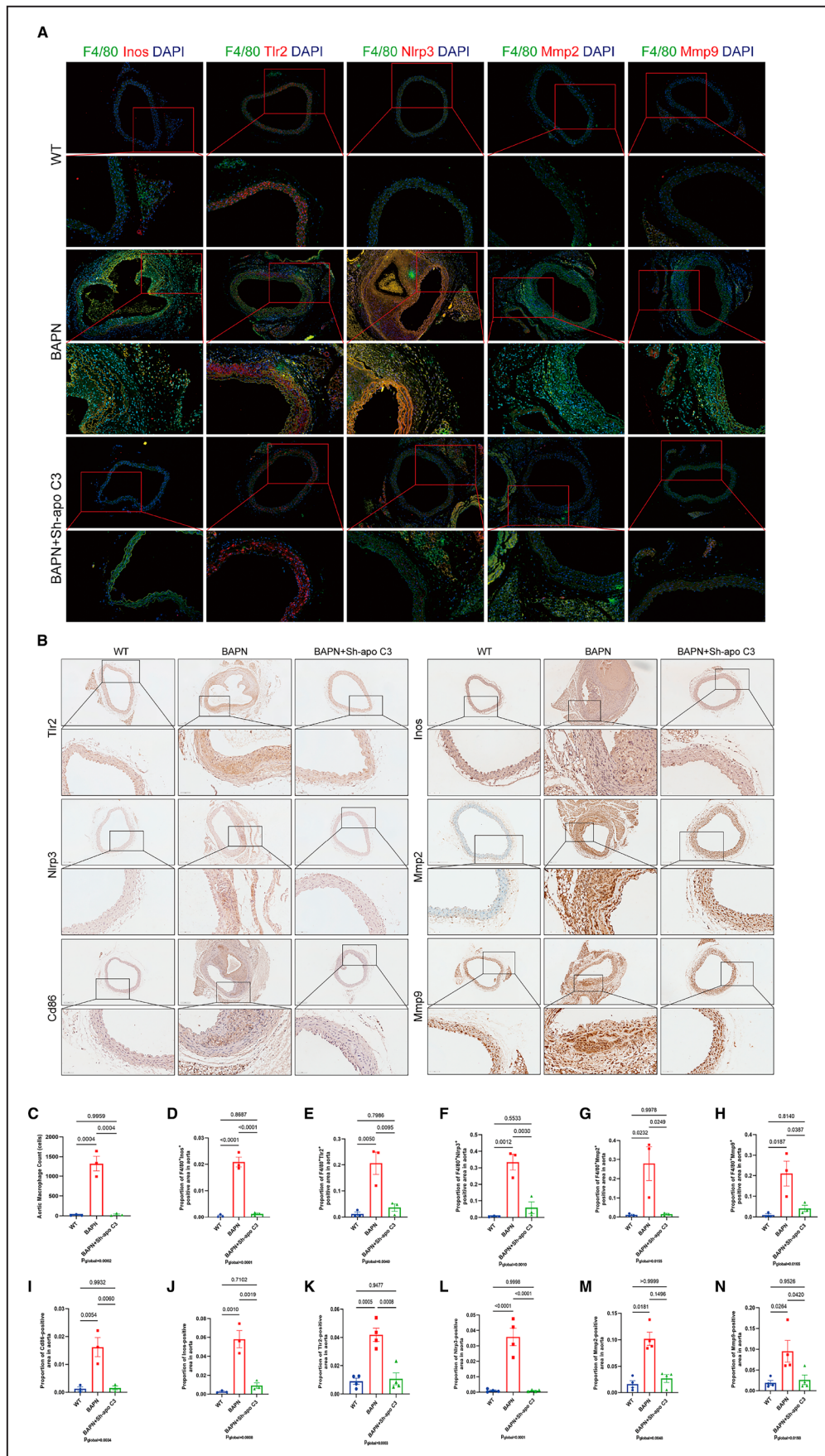
macrophage activation, and positive regulation of macrophage differentiation were affected after interference with hepatic apo C3 (Figure 3D). Kyoto Encyclopedia of Genes and Genomes analysis revealed that Toll-like receptor and NOD-like receptor signaling pathways were affected, and combining with heat map results, genes such as *Tlr2* and *Nlrp3* were downregulated in the BAPN+Sh-apo C3 group (Figure 3E). To further explore the specific sites of apo C3 action, we identified genes interacting with apo C3 on the basis of differential gene results in the STRING database (Figure 3C). Combining the above research results, we identified *Tlr2* as the most likely downstream gene of apo C3. Based on the GO analysis results, we focused on macrophage inflammatory responses. Therefore, we hypothesized that apo C3 promotes M1 macrophage polarization and *Mmps* release through the *Tlr2/Nlrp3* signaling pathway.

Hepatic Apo C3 Intervention Attenuates M1 Macrophage Polarization, Suppresses TLR2/NLRP3 Signaling Pathway Activation, and Diminishes MMP Release in Aortic Dissection

The immunofluorescence results revealed a significant presence of M1 macrophages (CD68⁺INOS⁺) in the aortas of patients with AD. These macrophages showed activation of the TLR2/NLRP3 pathway, with elevated levels of MMP2 and MMP9 proteins (Figure 4A through 4F). Consistent with the immunofluorescence findings, WB analysis demonstrated significantly increased levels of CD86, INOS, TLR2, NLRP3, MMP2, and MMP9 proteins in the aortas of patients with AD (Figure 4G through 4M). Similar results were obtained from immunohistochemistry and immunofluorescence analyses of mouse aortas (Figure 5A and 5B). Notably, intervention with hepatic apo C3 significantly reduced the number of macrophages in the aorta (Figure 5C), particularly M1 macrophages (Figure 5D, 5I, and 5J), accompanied by decreased activation of the TLR2/NLRP3 pathway and reduced release of MMP2 and MMP9 (Figure 5E through 5H and 5K through 5N).

Figure 5. The aortas of AD mice exhibit abundant M1 macrophages, with significant activation of the TLR2/NLRP3 signaling pathway, and increased release of MMP2 and MMP9.

However, this is alleviated after interfering with hepatic apo C3. Representative immunofluorescence (A) from aortas of each group of mice, with quantification of INOS (D), TLR2 (E), NLRP3 (F), MMP2 (G), and MMP9 (H) expression in the aortas of each group of mice ($n=3$ per group). (C) The number of aortic macrophages in each group of mice. Representative immunohistochemistry (B) from aortas of each group of mice, with quantification of CD86 (I), INOS (J), TLR2 (K), NLRP3 (L), MMP2 (M), and MMP9 (N) expression in the aortas of each group of mice ($n=4$ per group). Data are presented as mean \pm SEM. Bars represent the means, and caps represent the SEM. Statistical significance was determined by Kruskal–Wallis test with Dunn's multiple comparison test in M, and determined by 1-way ANOVA with Tukey's multiple comparisons test in C through L and N. A value of $P<0.05$ was considered significant. AD indicates aortic dissection; apo C3, apolipoprotein C3; CD, cluster of differentiation; INOS, inducible nitric oxide synthase; MMP, matrix metalloproteinase; NLRP3, NOD-like receptor pyrin domain containing 3; and TLR2, Toll-like receptor 2.



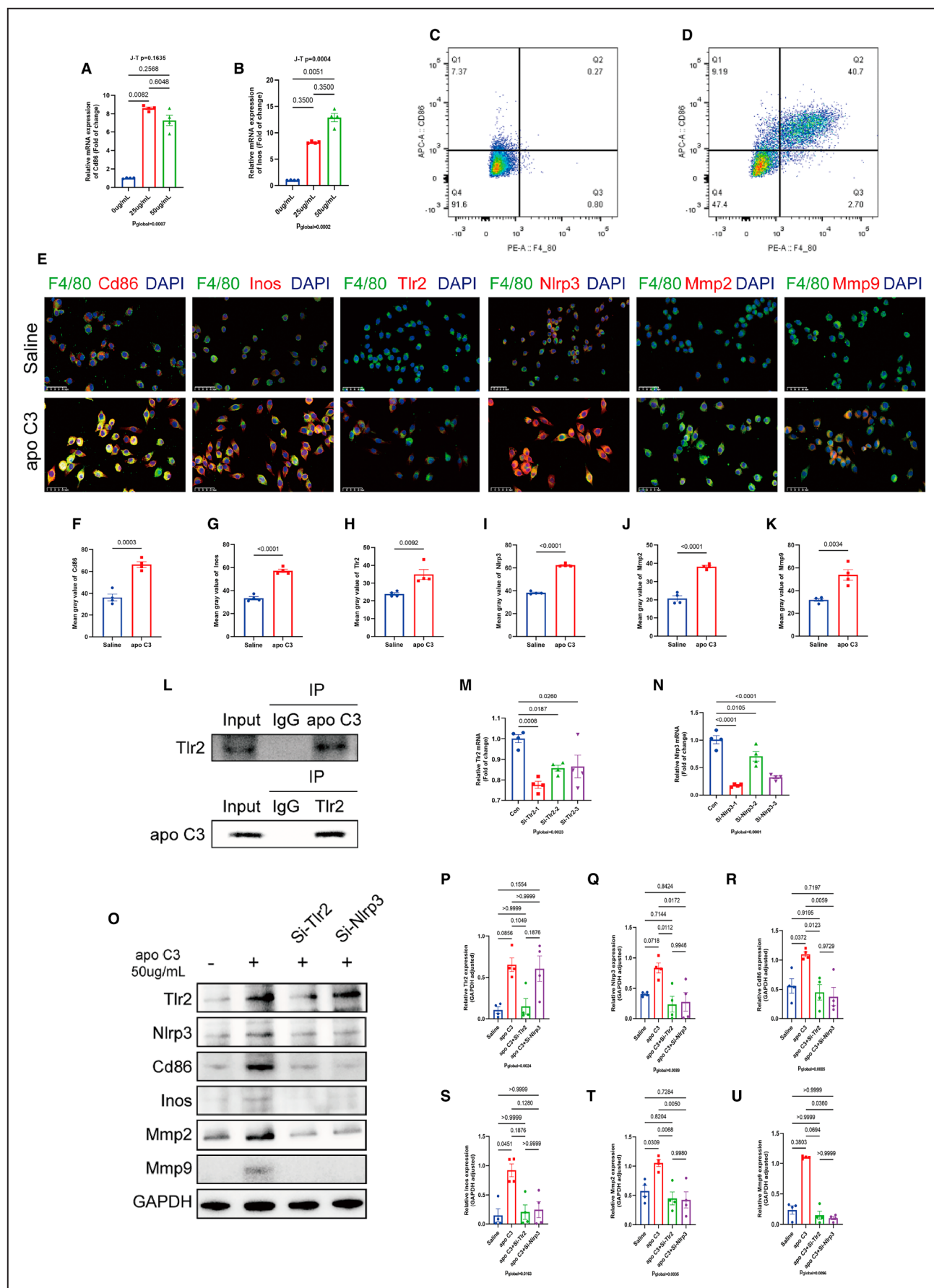


Figure 6. In vitro studies show apo C3 activates M1 polarization and MMPs secretion in macrophages via the TLR2/NLRP3 signaling pathway.

J774A.1 cells were divided into 4 groups: saline group, apo C3 group, apo C3+Si-TLR2 group, and apo C3+Si-NLRP3 group. Except for the saline group treated with saline, all other groups were treated with 50 µg/mL apo C3 for 48 h. **A** and **B**, mRNA levels of M1 macrophage markers CD86 and INOS in each group (n=4 per group). **C** and **D**, Flow cytometry analysis of CD86 and INOS protein expression in each group. Representative immunofluorescence (**E**) from the apo C3 group and saline group cells, quantification of CD86 (**F**), INOS (**G**), TLR2 (**H**), NLRP3 (**I**), MMP2 (**J**), and MMP9 (**K**) expression in the apo C3 group (n=4) and saline group (n=4) cells. **L**, Coimmunoprecipitation results of apo C3 and TLR2 protein interaction. **M** and **N**, mRNA levels of TLR2 and NLRP3 after interference with Si-TLR2 and Si-NLRP3. Representative western blot (**O**) from each group (n=4 from each group), quantification of TLR2 (**P**), NLRP3 (**Q**), CD86 (**R**), INOS (**S**), MMP2 (**T**), and MMP9 (**U**) expression in each group. Data are expressed as mean±SEM. Bars represent the means, and caps represent the SEM. Statistical significance was determined by Kruskal–Wallis test with Dunn's multiple comparison test in **A**, **B**, **P**, **S**, and **U**, and by Jonckheere–Terpstra test to evaluate the monotonic trend in **A** and **B**. Unpaired t test was used in **F** through **K**, and 1-way ANOVA with Tukey's multiple comparisons test was used in **M**, **N**, **Q**, **R**, and **T**. A value of $P<0.05$ was considered significant. apo C3 indicates apolipoprotein C3; CD, cluster of differentiation; INOS, inducible nitric oxide synthase; MMP, matrix metalloproteinase; NLRP3, NOD-like receptor pyrin domain containing 3; and TLR2, Toll-like receptor 2.

In Vitro Studies Show Apo C3 Activates M1 Polarization and MMP Secretion in Macrophages via the TLR2/NLRP3 Signaling Pathway

To investigate the direct effects of apo C3 on macrophages, recombinant mouse apo C3 protein was added to the culture medium of J774A.1 macrophages for 48 hours. Results showed that 50 µg/mL of apo C3 increased mRNA levels of INOS and CD86 (markers of M1 polarization) in macrophages (Figure 6A and 6B). Flow cytometry analysis revealed a notable increase in the proportion of F4/80⁺CD86⁺ macrophages after treatment with 50 µg/mL apo C3 compared with the control group (Figure 6C and 6D). The immunofluorescence results showed upregulation of *Cd86*, *Inos*, *Tlr2*, *Nlrp3*, *Mmp2*, and *Mmp9* expression in macrophages stimulated with 50 µg/mL apo C3 (Figure 6E through 6K). These findings suggest that apo C3 promotes M1 polarization, activation of the TLR2/NLRP3 pathway, and secretion of MMP2 and MMP9 to some extent. STRING database analysis revealed an interaction between apo C3 and TLR2. Coimmunoprecipitation experiments confirmed this interaction: J774A.1 macrophages were treated with 50 µg/mL apo C3 for 48 hours, followed by total protein extraction. Immunoprecipitation with the apo C3 antibody yielded a protein complex, and WB analysis showed the presence of TLR2 protein in the complex. Conversely, immunoprecipitation with TLR2 antibody also revealed the presence of apo C3 protein in the complex. This indicates an interaction between apo C3 and TLR2 (Figure 6L). To investigate the relationship between apo C3-mediated TLR2/NLRP3 activation and M1 polarization and MMP secretion, we constructed Si-TLR2 and Si-NLRP3 to interfere with *Tlr2* and *Nlrp3* expression in J774A.1 macrophages, respectively. PCR results showed that Si-TLR2-1 and Si-NLRP3-1 had the highest interference efficiency, so they were chosen for subsequent experiments (Figure 6M and 6N). Four groups of cell experiments were established: saline

group, apo C3 group, apo C3+Si-TLR2 group, and apo C3+Si-NLRP3 group. Except for the saline group, all other groups were treated with 50 µg/mL apo C3 for 48 hours. WB results showed that apo C3 stimulation increased protein levels of CD86, INOS, TLR2, NLRP3, MMP2, and MMP9 in macrophages. Upon TLR2 interference, all protein levels significantly decreased, indicating that TLR2, as a key upstream regulator, affects M1 polarization and MMP2 and MMP9 secretion in macrophages. After NLRP3 interference, except for TLR2 protein expression, which showed no difference ($P>0.9999$), other protein levels significantly decreased, suggesting that NLRP3 acts downstream of TLR2 and regulates M1 polarization and MMP2 and MMP9 secretion in macrophages. Overall, apo C3 activates M1 polarization and MMP secretion in macrophages via the TLR2/NLRP3 signaling pathway (Figure 6O through 6U).

Inhibition of TLR2 With C29 Reduces Incidence of AD, Inhibits the TLR2/NLRP3 Pathway, Suppresses M1 Polarization, and Decreases MMP Secretion

To investigate the critical role of TLR2, a downstream molecule of apo C3, in the occurrence of AD, mice were intragastrically administered the TLR2 inhibitor C29 (25 mg/kg). The animal experiment was divided into 3 groups: WT group, BAPN group, and BAPN+C29 group. Results showed that after administration of C29, the incidence of AD decreased in mice (13/30) compared with the BAPN group (22/30) ($P=0.0352$) (Figure 7A). The survival curve results in Figure 7B show that the survival rate of mice in the BAPN+C29 group was higher at 28 days compared with the BAPN group ($P=0.0184$). This suggests that systemic inhibition of TLR2 can reduce AD deaths. At 8 weeks, the body weight of WT mice was significantly higher than that of the BAPN group ($P=0.0293$) and the BAPN+C29 group ($P=0.0237$). However, there was no significant difference in body weight

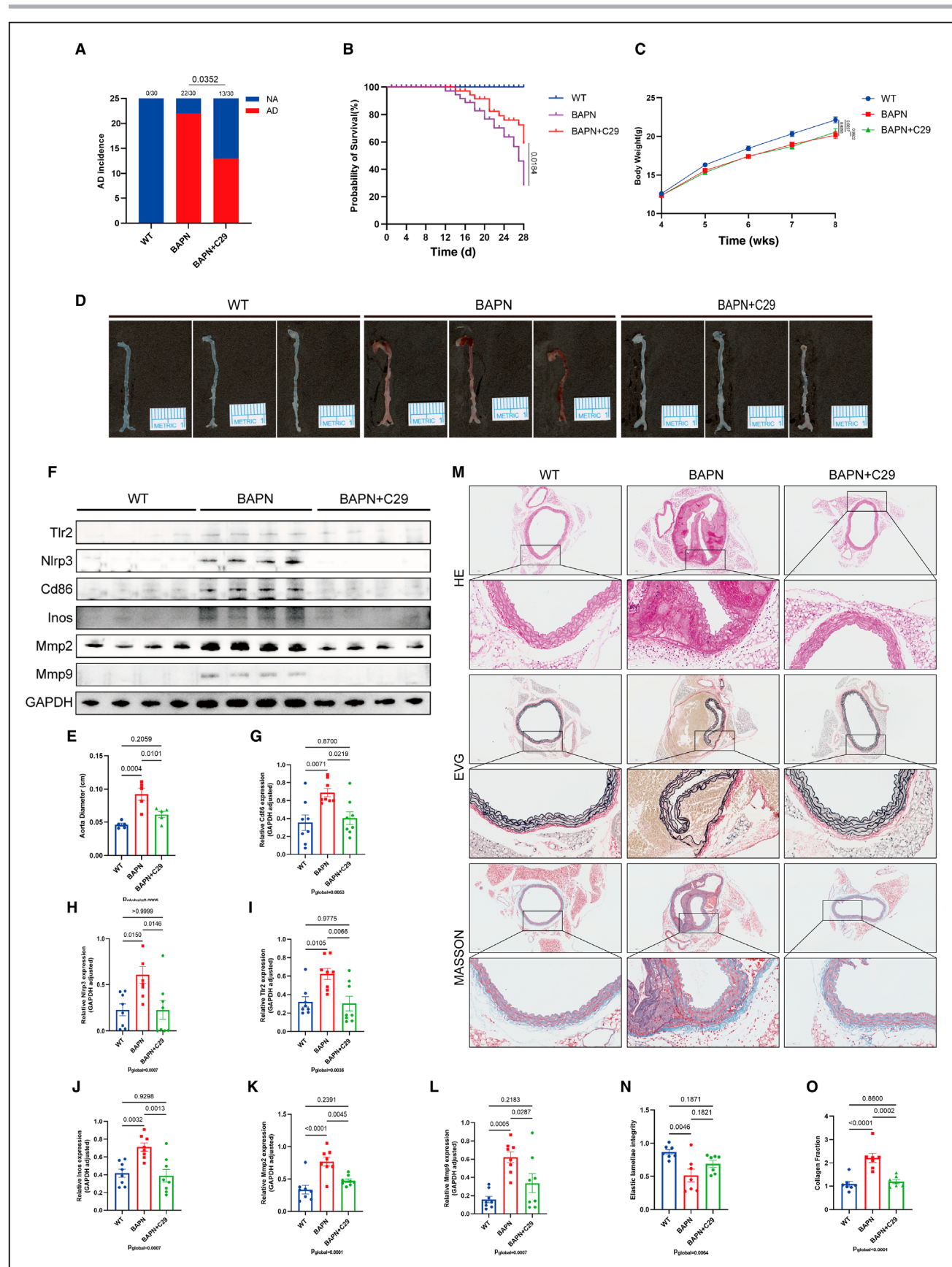


Figure 7. The TLR2 inhibitor C29 reduced the incidence of AD, suppressed M1 polarization, blocked the TLR2/NLRP3 signaling pathway and decreased MMP secretion.

The animal experiment was divided into 3 groups: WT group, BAPN group, and BAPN+C29 group. The BAPN+C29 group received intragastric administration of 25 mg/kg C29 for 4 weeks. **A**, Incidence of AD in each group (n=30 per group). **B**, Survival curves of mice in each group (n=30 per group). **C**, Body weight curves of mice in each group (n=30 per group). **D**, Representative aortic images from each group. **E**, The aortic diameter of each group of mice (n=5 per group). Representative western blot (**F**) from each group (n=8 from each group), quantification of CD86 (**G**), NLRP3 (**H**), TLR2 (**I**), INOS (**J**), MMP2 (**K**), and MMP9 (**L**) expression in each group. **M**, Representative images of HE staining, EVG staining, and Masson staining of aortas from each group (n=7 per group). **N** and **O**, Quantification of elastic fiber and collagen fiber areas in aortic histological staining (**M**) from each group. Comparisons of AD incidence were analyzed using Fisher's exact test (**A**). Comparisons of survival curves were analyzed using the log-rank test (**B**). One-way ANOVA with Tukey's multiple comparisons test was used in **E**, **G** through **L**, **N**, and **O**. Data are expressed as mean±SEM. Bars represent the means, and caps represent the SEM. A value of $P<0.05$ was considered significant. AD indicates aortic dissection; BAPN, β -aminopropionitrile; CD, cluster of differentiation; EVG, Elastic Van Gieson; HE, hematoxylin and eosin; INOS, inducible nitric oxide synthase; MMP, matrix metalloproteinase; NLRP3, NOD-like receptor pyrin domain containing 3; TLR2, Toll-like receptor 2; and WT, wild-type.

between the BAPN group and the BAPN+C29 group ($P=0.8622$) (Figure 7C). Figure 7D shows representative images of aortas from each group. Figure 7E shows the differences in maximum aortic diameter among the different mouse groups. The results indicate that the maximum aortic diameter in the BAPN+C29 group was significantly smaller than that in the BAPN group ($P=0.0101$), but there was no significant difference compared with the WT group ($P=0.2059$). This suggests that systemic inhibition of TLR2 can reduce aortic dilation induced by AD modeling. WB results demonstrated that inhibition of TLR2 by C29 suppressed the expression of NLRP3, CD86, INOS, MMP2, and MMP9 proteins (Figure 7F through 7L). These findings suggest that inhibition of TLR2 not only suppresses downstream molecule NLRP3 but also inhibits M1 polarization and MMP secretion in macrophages. Histological staining results of mouse aortas showed that, compared with the BAPN group, the BAPN+C29 group exhibited a more intact aortic structure, with reduced elastic fiber fragmentation ($P=0.1821$, although not statistically significant) and decreased collagen deposition ($P=0.0002$) (Figure 7M through 7O). This indicates a significant improvement in extracellular matrix degradation following TLR2 inhibition. Taken together, these results suggest that the downstream molecule of apo C3, TLR2, plays a crucial role in the occurrence of AD.

Apo C3 Promotes Inflammation, Chemotaxis, and Apoptosis in Aortic Vascular Smooth Muscle Cells

Due to the deposition of apo C3 in the aorta and the crucial role of aortic vascular smooth muscle cells as the major component of the aorta in the occurrence of AD, we investigated the effects of apo C3 on MOVAS. Mouse recombinant apo C3 protein was added to MOVAS culture medium and incubated for 48 hours, with physiological saline given to the control group. Then, we performed transcriptome sequencing on these 2 groups of cells. The volcano plot showed

that among the differentially expressed genes, 212 genes were upregulated and 88 genes were downregulated (Figure 8A). The heat map results demonstrated upregulation of TLR2, CC chemokine ligand family (CCL2, CCL20, CCL5, and CCL7), C-X-C motif chemokine ligand family (CXCL1, CXCL2, and CXCL5), and inflammatory proteins (interleukin-6 and serum amyloid A3) (Figure 8B). GO analysis indicated that apo C3 promoted inflammation, adhesion, and chemotaxis in MOVAS (Figure 8C). Kyoto Encyclopedia of Genes and Genomes analysis revealed the involvement of chemokine signaling pathways, Toll-like receptor signaling pathways, and NOD-like receptor signaling pathways (Figure 8D). PCR validation of some key genes showed upregulation of CXCL1, CXCL5, CCL2, CCL7, serum amyloid A3, and interleukin-6 mRNA levels and the expression of these genes increased with increasing concentrations of apo C3. (Figure 8E). Since MOVAS phenotypic transformation is one of the main mechanisms underlying AD, we assessed the phenotypic markers of MOVAS after apo C3 intervention. The results showed no significant change in the contractile marker α -smooth muscle actin, while the secretory marker osteopontin was downregulated, indicating that apo C3 intervention did not induce a shift from a contractile to a synthetic phenotype in MOVAS (Figure 8F and 8G). We further investigated the effects of apo C3 on MOVAS function. Cell-Counting Kit-8 results demonstrated that MOVAS proliferation was inhibited at 24 hours ($P=0.0032$) and 48 hours ($P=0.0230$) after treatment with 50 μ g/mL apo C3 (Figure 8H). Scratch assays similarly showed that the healing ability of MOVAS treated with 50 μ g/mL apo C3 was lower than that of the control group at 24 hours ($P<0.0001$) (Figure 8I and 8L). 5-Ethynyl-2'-deoxyuridine experiments yielded similar results ($P=0.0016$) (Figure 8J and 8M), suggesting that apo C3 inhibited MOVAS proliferation and migration. Terminal deoxynucleotidyl transferase dUTP nick-end labeling assays revealed that treatment with 50 μ g/mL apo C3 for 48 hours promoted MOVAS apoptosis ($P=0.0014$) (Figure 8K and 8N).

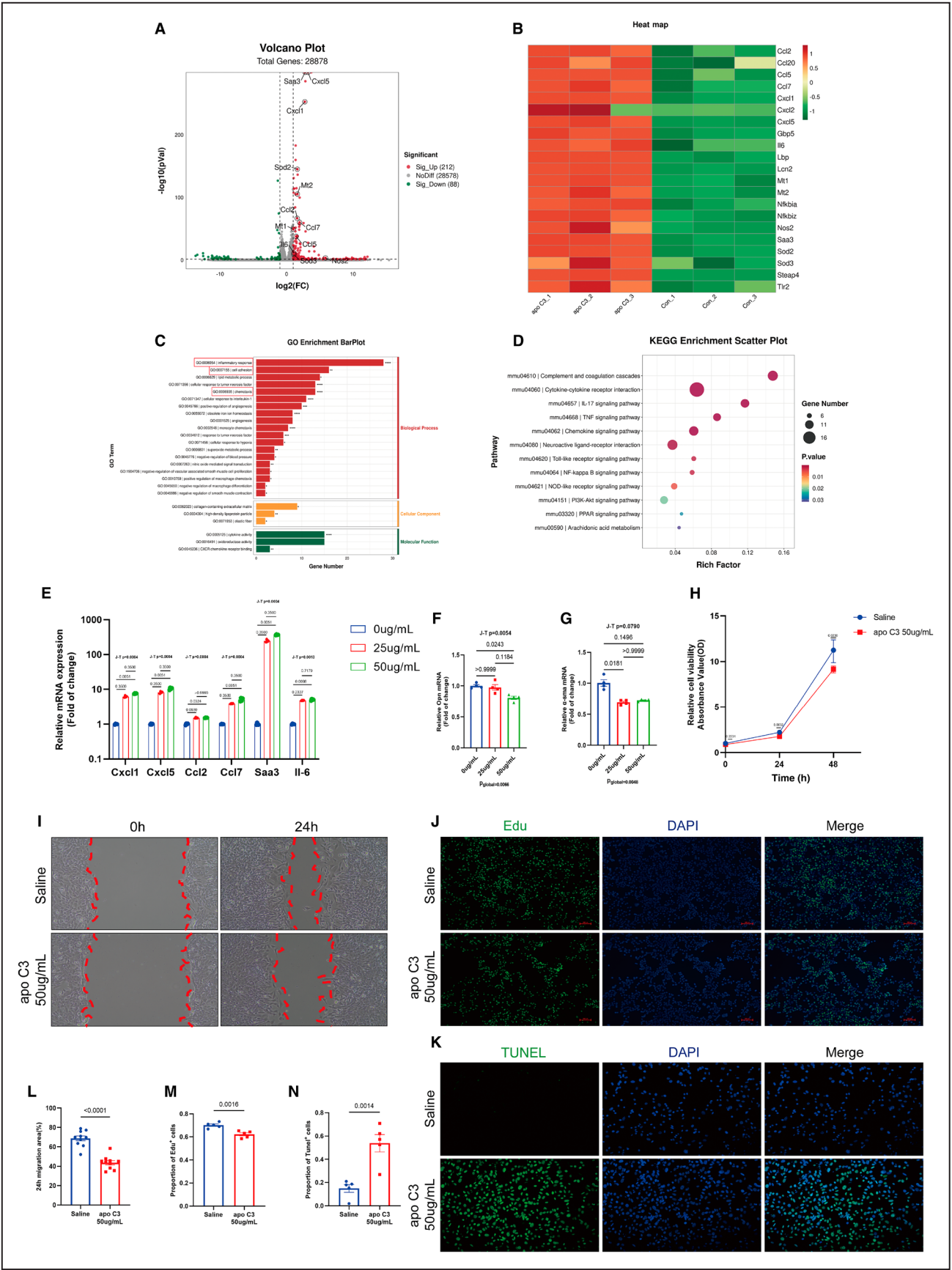


Figure 8. Apo C3 promotes inflammation, chemotaxis, and apoptosis of MOVAS cells.

MOVAS were treated with apo C3 at concentrations of 0 μ g/mL (saline), 25 μ g/mL, and 50 μ g/mL for 48 hours. RNA was extracted from the saline group and the 50 μ g/mL apo C3 group for transcriptome sequencing. **A**, Volcano plot. **B**, Heat map. **C**, GO analysis results. **D**, KEGG analysis results. **E**, mRNA levels of (Cxcl 1, Cxcl5, Ccl2, Ccl7, Saa3, and interleukin 6 in MOVAS under apo C3 concentration gradient intervention (n=4 per group). **F** and **G**, mRNA levels of osteopontin and α -SMA, representing phenotypes of MOVAS under apo C3 concentration gradient intervention (n=4 per group). **H**, Cell-Counting Kit-8 results of MOVAS in the saline group and the 50 μ g/mL apo C3 group (n=4 per group). **I**, Representative images of wound healing experiments in the saline group (n=9) and the 50 μ g/mL apo C3 group (n=9), with quantitative analysis of migration area (L) in each group. **J**, Representative images of Edu staining in the saline group (n=5) and the 50 μ g/mL apo C3 group (n=5), with quantitative analysis of the proportion of Edu-positive cells (**M**) in each group. **K**, Representative images of terminal deoxynucleotidyl transferase dUTP nick-end labeling staining in the saline group (n=5) and the 50 μ g/mL apo C3 group (n=5), with quantitative analysis of the proportion of terminal deoxynucleotidyl transferase dUTP nick-end labeling-positive cells (**N**) in each group. Data are expressed as mean \pm SEM. Bars represent the means, and caps represent the SEM. Kruskal–Wallis test with Dunn’s multiple comparison test and Jonckheere–Terpstra test was used in **E** through **G**, and unpaired *t* test was used in **L** through **N**. A value of *P*<0.05 was considered significant. Apo C3 indicates apolipoprotein C3; Ccl, C-c motif chemokine ligand; Cxcl, C-x-c motif chemokine ligand; IL-6, interleukin 6; GO, gene ontology; KEGG, Kyoto Encyclopedia of Genes and Genomes; MOVAS, mouse aortic vascular smooth; Saa3, Serum amyloid A3; α -SMA, α -smooth muscle actin; and TUNEL, terminal deoxynucleotidyl transferase dUTP nick-end labeling.

Apo C3 Promotes Expression of Adhesion Molecules in Aortic Endothelial Cells to Facilitate Macrophage Adhesion

Due to the deposition of apo C3 in the endothelial and subendothelial layers of the aorta, we investigated the direct effects of apo C3 on MAECs. PCR results showed that treatment of MAECs with different concentrations of apo C3 for 48 hours resulted in increased mRNA levels of vascular cell adhesion molecule 1, intercellular adhesion molecule 1, and E-selectin, while the mRNA level of platelet endothelial cell adhesion molecule-1 decreased or remained unchanged (Figure 9A). The expression levels of intercellular adhesion molecule 1 and E-selectin increased with increasing concentrations of apo C3. The results of the macrophage adhesion assay showed that at 1 minute and 5 minutes, the adhesion ratio of macrophages after apo C3 intervention (apo C3 1-minute group and apo C3 5-minute group) to ECs was significantly higher than that of the untreated groups (saline 1-minute group and saline 5-minute group; Figure 9B and 9D). These results suggest that apo C3 enhances the adhesion ability of ECs. We have provided a schematic diagram of the mechanism of this study in Figure 9E.

DISCUSSION

This article first discovered that apo C3 is abnormally elevated in the plasma exosomes of patients with AD. It was then found and confirmed that apo C3 is highly expressed in the plasma and aortas of patients with AD. Interestingly, apo C3 mRNA was undetectable in the aortic mRNA of both patients with AD and NCs, suggesting that the deposited apo C3 in the aorta does not originate from the aorta itself. A Mouse AD model was constructed by feeding BAPN to verify the high expression of apo C3 in the plasma and aortic wall of mice. The mRNA expression levels of apo C3 in the aortas of

AD mice and controls were extremely low and showed no statistical difference. Additionally, liver apo C3 levels were higher in the BAPN group compared with the control group. When liver apo C3 was knocked down, plasma and aortic apo C3 levels decreased, indicating that the apo C3 in the aortas of AD mice was secreted in large amounts by the liver and then deposited in the aorta via the bloodstream. Importantly, the incidence of AD significantly decreased in mice with liver apo C3 knockdown, and improvements in elastic fiber integrity and collagen deposition were observed, suggesting that apo C3 plays a promotive role in the development of AD.

To further elucidate the mechanism of apo C3 in the development of AD, we conducted transcriptome sequencing on the aortas of mice from the BAPN group and the BAPN+Sh-apo C3 group. The results indicated that interference with hepatic apo C3 led to the downregulation of M1 macrophage markers CD86 and iNOS in the aorta, as well as the downregulation of MMP2 and MMP9. Additionally, the Toll-like receptor and NOD-like receptor signaling pathways were suppressed. Using the STRING database, we discovered an interaction between apo C3 and the TLR2 receptor, suggesting that apo C3 may enhance M1 macrophage polarization and stimulate the release of MMP2 and MMP9 via the TLR2/NLRP3 signaling pathway. To validate this hypothesis, we confirmed that during the occurrence of AD, there is a significant presence of M1 macrophages on both human and mouse aortas, with these cells exhibiting significant activation of the TLR2/NLRP3 signaling pathway and increased release of MMP2 and MMP9. However, when hepatic apo C3 interference was introduced in mice, this process was inhibited. Next, we added apo C3 recombinant protein to the culture medium of J774A.1 cells. The results showed that apo C3 promoted macrophage M1 polarization, activated the TLR2/NLRP3 signaling pathway, and enhanced the release of MMP2 and MMP9.

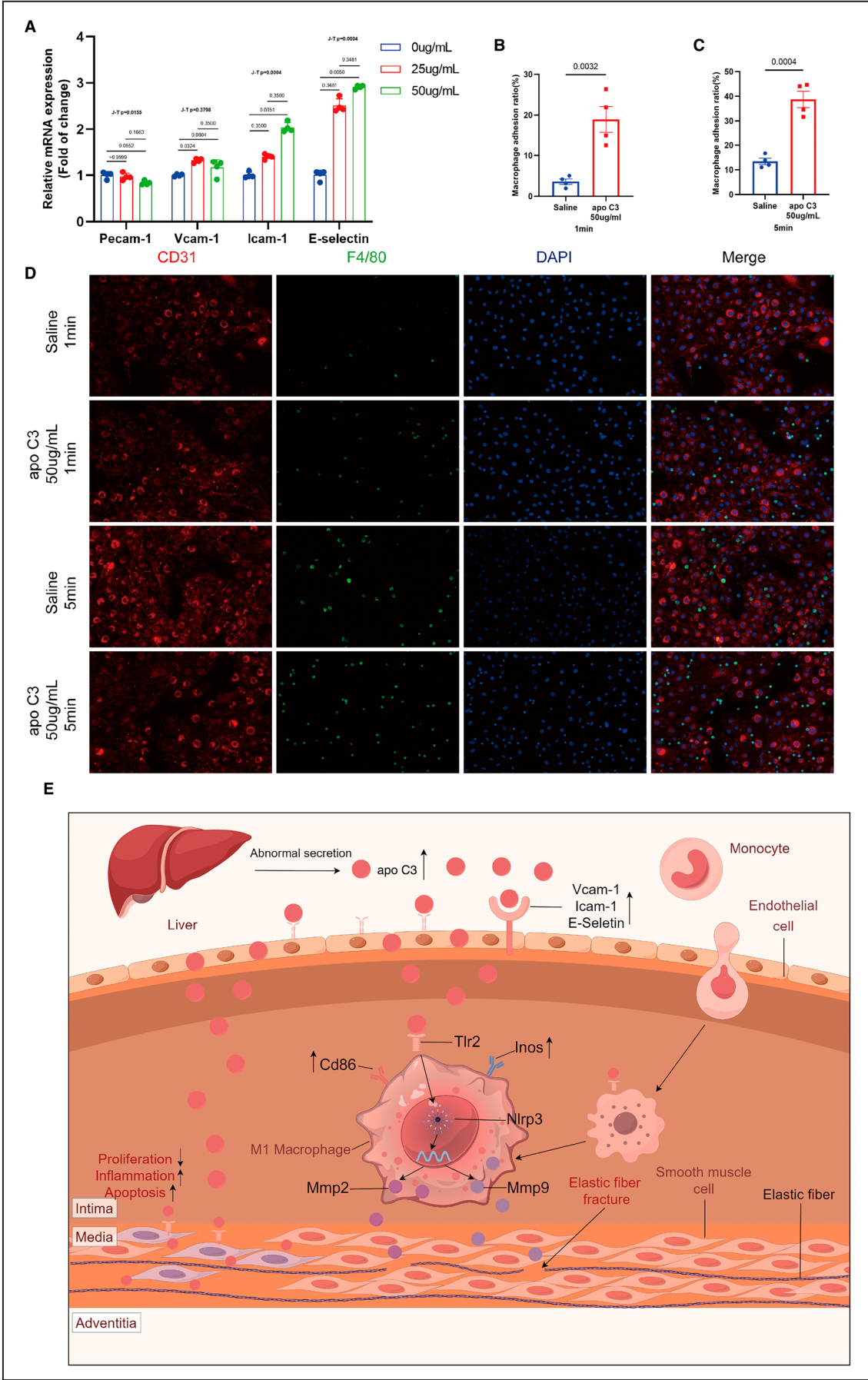


Figure 9. Apo C3 promotes the expression of adhesion molecules in MAECs, leading to increased macrophage adhesion.

MAECs were treated with apo C3 at concentrations of 0 μ g/mL (saline), 25 μ g/mL, and 50 μ g/mL for 48 h. **A**, mRNA levels of adhesion molecules PECAM-1, VCAM-1, ICAM-1, and E-selectin in MAECs under different concentrations of apo C3 intervention (n=4 per group). **D**, Representative images of macrophage adhesion experiment in different groups. **B** and **C**, Quantification of macrophage adhesion ratio at 1 and 5 min, respectively (n=4 per group). **E**, Mechanism diagram of this study. Data are expressed as mean \pm SEM. Bars represent the means, and caps represent the SEM. Kruskal–Wallis test with Dunn's multiple comparison test and Jonckheere–Terpstra test was used in (**A**), and unpaired *t* test was used in **B** and **C**. A value of *P*<0.05 was considered significant. Apo C3 indicates apolipoprotein C3; ICAM-1, intercellular adhesion molecule-1; MAEC, mouse aortic endothelial cell; PECAM-1, platelet endothelial cell adhesion molecule-1; and VCAM-1, vascular cell adhesion molecule-1.

To elucidate the specific mechanism by which apo C3 influences macrophage M1 polarization, we first conducted coimmunoprecipitation experiments for TLR2 and apo C3, confirming the interaction between TLR2 and apo C3. Subsequently, we used siRNA to silence TLR2 and NLRP3 in J774A.1 cells while concurrently stimulating the cells with apo C3 recombinant protein. The results indicated that knockdown of TLR2 and NLRP3 inhibited apo C3-induced macrophage M1 polarization and MMP release. Furthermore, when TLR2 was knocked down, NLRP3 levels decreased. However, when NLRP3 was knocked down, TLR2 levels remained unchanged, indicating that NLRP3 acts as a downstream molecule of TLR2. Through animal experiments, we found that the TLR2 inhibitor C29 can reduce the incidence of AD, inhibit macrophage M1 polarization, suppress the TLR2/NLRP3 pathway, and decrease the secretion of MMPs. This also demonstrates the critical role of the TLR2/NLRP3 signaling pathway in AD. Overall, apo C3 promotes macrophage M1 polarization and the secretion of MMP2 and MMP9 by binding to TLR2 on the macrophage membrane and activating the NLRP3 inflammasome, thereby enhancing aortic inflammation and extracellular matrix degradation.

Given the critical role of MOVAS in the development of AD, we also investigated the effect of apo C3 on MOVAS by adding apo C3 to MOVAS culture medium and conducting transcriptome sequencing compared with the control group. The results suggested that apo C3 enhanced inflammation, cell adhesion, and chemotaxis in MOVAS, and we validated some key indicators, obtaining consistent results. Furthermore, we explored the functional impact of apo C3 on MOVAS through cellular functional assays, finding that apo C3 inhibited MOVAS proliferation and migration while promoting apoptosis, aligning with the pathogenesis of AD. Unfortunately, the phenotypic transformation of MOVAS cocultured with apo C3 was not significantly affected. Finally, we assessed the effect of apo C3 on the function of MAECs, observing an upregulation of adhesion molecules such as vascular cell adhesion molecule 1 and intercellular adhesion molecule 1. Macrophage adhesion experiments demonstrated that MAECs pretreated with apo C3 had an increased capacity for macrophage adhesion.

In summary, our study revealed that excessive secretion of apo C3 by the liver results in its deposition on the aorta, promoting adhesion of endothelial cells and blood-derived monocytes. Apo C3 also enhances macrophage M1 polarization and smooth muscle cell inflammation, thereby inducing aortic inflammation. Additionally, apo C3 stimulates macrophages to secrete MMP2 and MMP9, which contribute to the degradation of the aortic extracellular matrix. Additionally, apo C3 inhibits smooth muscle cell proliferation and promotes apoptosis of smooth muscle cells, leading to the loss of medial smooth muscle cells in the aorta. These findings elucidate part of the mechanisms by which apo C3 contributes to the development of AD. We hope that apo C3 can serve as a novel therapeutic target, offering new approaches for the treatment of AD.

There are many factors that influence the synthesis and secretion of apo C3 by the liver, and here we will analyze the factors that may promote the synthesis and secretion of apo C3 in the process of AD occurrence.

1. Insulin resistance and hyperglycemia. Studies have shown that insulin promotes the binding of forkhead box O1 to the apo C3 promoter, leading to upregulation of its expression, while insulin phosphorylation prevents forkhead box O1 translocation to the nucleus, thereby down-regulating apo C3 expression.¹⁷ Moreover, apo C3 levels are significantly elevated in animal models of insulin resistance or deficiency. Our previous research has shown that nearly 60% of patients with acute thoracic AD exhibit insulin resistance.¹⁸ Additionally, glucose can promote hepatic apo C3 expression through carbohydrate response element-binding protein and hepatocyte nuclear factor-4.¹⁹ Studies have shown that nearly 40% of patients with acute thoracic AD experience stress-induced hyperglycemia without a history of diabetes.²⁰ Therefore, widespread insulin resistance and hyperglycemia observed in patients with AD may serve as one of the main reasons for increased hepatic secretion of apo C3.
2. Inflammatory response. Studies have shown elevated serum levels of apo C3 in some

autoimmune diseases such as rheumatoid arthritis and systemic lupus erythematosus, suggesting that inflammatory responses may promote the secretion of apo C3 through certain pathways.^{21,22} Elevated apo C3 levels can further amplify inflammation by activating the NLRP3 inflammasome to participate in sterile inflammation.²³

3. Estrogen levels. Studies have shown a negative correlation between estrogen and apo C3 levels.²⁴ This may explain why there is a higher prevalence of AD in men compared with women and why the incidence of AD is lower in premenopausal women. Elevated levels of estrogen in women suppress the synthesis and secretion of apo C3, reducing the likelihood of sterile inflammatory diseases.

Why does liver-secreted apo C3 deposit on the aorta? Our experimental results indicate that apo C3 primarily deposits in the endothelial layer and subendothelial layer of the aorta, similar to the deposition of lipoproteins in atherosclerosis. Studies have shown that apo C3 and apo B deposit in the subendothelial layer and colocalize with macrophages in diabetes-induced atherosclerosis.²⁵ Therefore, we hypothesize that the deposition of apo C3 in the aorta is similar to the lipid deposition process in atherosclerosis, likely caused by endothelial dysfunction or transcytosis-mediated lipoprotein deposition.²⁶ Additionally, lipoproteins in atherosclerosis are mainly composed of oxidized low-density lipoprotein. As a type of triglyceride-rich lipoprotein, low-density lipoprotein is rich in apo C3.²⁷ Based on the above findings, we propose that apo C3 also deposits in the subendothelial layer during the development of AD. Of course, this conclusion still needs to be validated through additional methods in future research.

What is the relationship between apo C3-positive regions and AD lesions? In this study, apo C3 deposition was primarily observed in the endothelial layer and subendothelial layer, whereas the typical site of AD lesions is mainly in the media. Although this may seem to lack a direct connection, apo C3 actually plays an indirect promotive role in AD lesions. It is well known that AD arises from multiple complex factors, such as hypertension, endothelial injury, smooth muscle cell phenotypic transformation, and macrophage inflammation. Our research indicates that apo C3 enhances EC adhesion, smooth muscle cell inflammation, chemotaxis, and apoptosis. More importantly, apo C3 can induce M1 macrophage polarization and the release of MMPs, leading to the degradation of elastin fibers in the media. These results suggest that apo C3, as one of the complex pathogenic factors in AD, promotes AD lesions through various mechanisms.

Apo C3 is a therapeutic target for lowering plasma triglyceride levels. Common lipid-lowering drugs used in clinical practice, such as fibrates, niacin, and statins, can only modestly reduce apo C3 levels (<30%).¹⁰ Therefore, developing drugs that specifically reduce apo C3 levels is particularly important. Antisense oligonucleotides work by binding to their target mRNA, leading to the degradation of the target RNA by RNase H1, thereby reducing the levels of the target protein.²⁸ Volanesorsen, a second-generation antisense oligonucleotide, can lower apo C3 levels by ~80% and triglyceride levels by 70% in patients with hypertriglyceridemia.²⁹ Olezarsen, another antisense oligonucleotide, can significantly alter the lipid profile in patients with atherosclerosis.³⁰ Additionally, ARO-apo C3, an siRNA, can reduce apo C3 levels by up to 94% and triglyceride levels by 74%.³¹ However, these apo C3-specific inhibitors have not been tested in AD and require animal studies and clinical trials to validate their effectiveness in specifically reducing apo C3 levels.

To our knowledge, this study is the first to report excessive hepatic secretion of apo C3 leading to its deposition in the aorta via plasma, thereby promoting AD. The experimental results revealed that abnormal hepatic secretion of apo C3 induces aortic inflammation, leading to the development of AD, suggesting a potential “cross-talk” between the liver and the aorta. Interfering with apo C3 in the liver and systemic TLR2 in mice can reduce the incidence of AD, suggesting that apo C3 and TLR2 can serve as targets for AD prevention with potential clinical implications. This study elucidates how apo C3 promotes macrophage M1 polarization and MMP secretion through the TLR2/NLRP3 pathway, partially revealing the proinflammatory mechanism of apo C3.

However, this study has several limitations. First, it did not verify whether the abnormal elevation of plasma apo C3 is solely due to the increase in exosomal apo C3 levels. Second, although the study initially planned to use AAV vectors to overexpress apo C3 in the mouse liver, the high baseline expression of apo C3 in the liver made further overexpression impossible, leading to incomplete findings in this regard. Third, specific inhibitors of apo C3, such as antisense oligonucleotides and siRNA, were not used to interfere with hepatic apo C3. Fourthly, most experiments in this study compared the BAPN group with the BAPN+Sh-apo C3 group, but the actual control group for the BAPN+Sh-apo C3 group should have been the BAPN+Sh-NC group. Although there were no significant differences in AD incidence, plasma apo C3 levels, and hepatic apo C3 levels between the BAPN and BAPN+Sh-NC groups, the role of AAV in the liver was not considered. Fifth, the sample size in some of the experiments was relatively small, which could affect the statistical power of the tests. We plan to increase the sample size in future studies to

improve the reliability and robustness of the findings. Finally, the elevated apo C3 in WT mice may induce a proinflammatory state, which needs further experimental validation. We plan to address these limitations in future experiments.

CONCLUSIONS

Our findings indicate that the deposition of apo C3 in the aorta is attributed to abnormal hepatic secretion. Apo C3 activates the TLR2/NLRP3 pathway to induce M1 polarization of macrophages and the secretion of MMPs. Furthermore, apo C3 promotes the expression of adhesion molecules in endothelial cells and enhances inflammation, chemotaxis, and apoptosis in aortic vascular smooth muscle cells.

ARTICLE INFORMATION

Received June 17, 2024; accepted November 22, 2024.

Affiliations

Department of Cardiovascular Surgery, Fujian Medical University Union Hospital, Fuzhou, China (X.Z., M.Z., Y.S., Z.Z., J.H., L.X., Q.W., X.L., K.C., Y.T., Y.L., Y.Z., Z.C., Z.Q., L.C.); Key Laboratory of Cardio-Thoracic Surgery (Fujian Medical University), Fujian Province University, Fuzhou, China (X.Z., M.Z., Y.S., Z.Z., J.H., L.X., Q.W., X.L., K.C., Y.T., Y.L., Y.Z., Z.C., Z.Q., L.C.); and Fujian Provincial Center for Cardiovascular Medicine, Fuzhou, China (Z.C., Z.Q., L.C.).

Acknowledgments

The authors acknowledge the Instrumentation and Technical Support provided by the Public Technology Service Center Fujian Medical University. The mechanic diagram is drawn by Figdraw. Drs Zhuang and Cai participated in the design of the study, carried out experimentations and statistical analysis, and drafted the manuscript; Drs Zarif, Shen, and K. Chen participated in animal experiments; Drs Z. Zhang and Tian participated in cell experiments; Drs He, Lin, and Y. Zhang were responsible for specimen collection; Drs Xie, Wu, and X. Lin were responsible for collecting and analyzing clinical data; Drs L. Chen and Qiu conceptualized the study. All authors read and approved the final manuscript.

Sources of Funding

This work was supported by the National Natural Science Foundation of China (U2005202, 82241209, 82241210, 82370470, 82400300), Fujian Provincial Special Reserve Talents Fund (2021-25), Key Laboratory of Cardio-Thoracic Surgery (Fujian Medical University), Fujian Province University Construction Project (2019-67) and Fujian Provincial Center for Cardiovascular Medicine Construction Project (2021-76).

Disclosures

None.

Supplemental Material

Tables S1–S2
Figure S1

REFERENCES

- Hirst AE, Johns VJ, Kime SW. Dissecting aneurysm of the aorta: a review of 505 cases. *Medicine (Baltimore)*. 1958;37:217–279. doi: [10.1097/00005792-195809000-00003](#)
- Shen YH, LeMaire SA, Webb NR, Cassis LA, Daugherty A, Lu HS. Aortic aneurysms and dissections series. *Arterioscler Thromb Vasc Biol*. 2020;40:e37–e46. doi: [10.1161/ATVBAHA.120.313991](#)
- Zhou C, Lin Z, Cao H, Chen Y, Li J, Zhuang X, Ma D, Ji L, Li W, Xu S, et al. Anxa1 in smooth muscle cells protects against acute aortic dissection. *Cardiovasc Res*. 2022;118:1564–1582. doi: [10.1093/cvr/cvab109](#)
- Xia L, Sun C, Zhu H, Zhai M, Zhang L, Jiang L, Hou P, Li J, Li K, Liu Z, et al. Melatonin protects against thoracic aortic aneurysm and dissection through SIRT1-dependent regulation of oxidative stress and vascular smooth muscle cell loss. *J Pineal Res*. 2020;69:e12661. doi: [10.1111/jpi.12661](#)
- Cifani N, Proietta M, Tritapepe L, Di Gioia C, Ferri L, Taurino M, Del Porto F. Stanford-a acute aortic dissection, inflammation, and metalloproteinases: a review. *Ann Med*. 2015;47:441–446. doi: [10.3109/07853890.2015.1073346](#)
- del Porto F, Proietta M, Tritapepe L, Miraldi F, Koverech A, Cardelli P, Tabacco F, de Santis V, Vecchione A, Mitterhofer AP, et al. Inflammation and immune response in acute aortic dissection. *Ann Med*. 2010;42:622–629. doi: [10.3109/07853890.2010.518156](#)
- Saraff K, Babamusta F, Cassis LA, Daugherty A. Aortic dissection precedes formation of aneurysms and atherosclerosis in angiotensin II-infused, apolipoprotein E-deficient mice. *Arterioscler Thromb Vasc Biol*. 2003;23:1621–1626. doi: [10.1161/01.ATV.0000085631.76095.64](#)
- Luo F, Zhou X-L, Li J-J, Hui R-T. Inflammatory response is associated with aortic dissection. *Ageing Res Rev*. 2009;8:31–35. doi: [10.1016/j.arr.2008.08.001](#)
- Ramms B, Gordts PLSM. Apolipoprotein C-III in triglyceride-rich lipoprotein metabolism. *Curr Opin Lipidol*. 2018;29:171–179. doi: [10.1097/MOL.0000000000000502](#)
- Packard CJ, Pirillo A, Tsimikas S, Ference BA, Catapano AL. Exploring apolipoprotein C-III: pathophysiological and pharmacological relevance. *Cardiovasc Res*. 2024;119:2843–2857. doi: [10.1093/cvr/cvad177](#)
- Zheng C, Khoo C, Ikewaki K, Sacks FM. Rapid turnover of apolipoprotein C-III-containing triglyceride-rich lipoproteins contributing to the formation of LDL subfractions. *J Lipid Res*. 2007;48:1190–1203. doi: [10.1194/jlr.P600011-JLR200](#)
- Lee S-J, Campos H, Moye LA, Sacks FM. LDL containing apolipoprotein CIII is an independent risk factor for coronary events in diabetic patients. *Arterioscler Thromb Vasc Biol*. 2003;23:853–858. doi: [10.1161/01.ATV.0000066131.01313.EB](#)
- Talayero B, Wang L, Furtado J, Carey VJ, Bray GA, Sacks FM. Obesity favors apolipoprotein E- and C-III-containing high density lipoprotein subfractions associated with risk of heart disease. *J Lipid Res*. 2014;55:2167–2177. doi: [10.1194/jlr.M042333](#)
- Kawakami A, Aikawa M, Alcaide P, Lusinskas FW, Libby P, Sacks FM. Apolipoprotein CIII induces expression of vascular cell adhesion molecule-1 in vascular endothelial cells and increases adhesion of monocytic cells. *Circulation*. 2006;114:681–687. doi: [10.1161/CIRCULATIONAHA.106.622514](#)
- Hu X, Ding S, Lu G, Lin Z, Liao L, Xiao W, Ding Y, Zhang Y, Wang Z, Gong W, et al. Apolipoprotein C-III itself stimulates the Syk/cPLA2-induced inflammasome activation of macrophage to boost anti-tumor activity of CD8+ T cell. *Cancer Immunol Immunother*. 2023;72:4123–4144. doi: [10.1007/s00262-023-03547-8](#)
- Schunk SJ, Hermann J, Sarakpi T, Triem S, Lellig M, Hahm E, Zewinger S, Schmit D, Becker E, Möllmann J, et al. Guanidinylated Apolipoprotein C3 (ApoC3) associates with kidney and vascular injury. *J Am Soc Nephrol*. 2021;32:3146–3160. doi: [10.1681/ASN.2021040503](#)
- Altomonte J, Cong L, Harbaran S, Richter A, Xu J, Meseck M, Dong HH. Foxo1 mediates insulin action on apoC-III and triglyceride metabolism. *J Clin Invest*. 2004;114:1493–1503. doi: [10.1172/JCI200419992](#)
- Zheng H, Qiu Z, Chai T, He J, Zhang Y, Wang C, Ye J, Wu X, Li Y, Zhang L, et al. Insulin resistance promotes the formation of aortic dissection by inducing the phenotypic switch of vascular smooth muscle cells. *Front Cardiovasc Med*. 2021;8:732122. doi: [10.3389/fcvm.2021.732122](#)
- Caron S, Verrijken A, Mertens I, Samanez CH, Mautino G, Haas JT, Duran-Sandoval D, Prawitt J, Francque S, Vallez E, et al. Transcriptional activation of apolipoprotein CIII expression by glucose may contribute to diabetic dyslipidemia. *Arterioscler Thromb Vasc Biol*. 2011;31:513–519. doi: [10.1161/ATVBAHA.110.220723](#)
- Liu S, Song C, Cui K, Bian X, Wang H, Fu R, Zhang R, Yuan S, Dou K. Prevalence and prognostic impact of stress-induced hyperglycemia in patients with acute type a aortic dissection. *Diabetes Res Clin Pract*. 2023;203:110815. doi: [10.1016/j.diabres.2023.110815](#)
- Martín-González C, Martín-Folgueras T, Quevedo-Abeledo JC, de Armas-Rillo L, González-Gay MÁ, Ferraz-Amaro I. Disease activity

- in patients with rheumatoid arthritis increases serum levels of apolipoprotein C-III. *Clin Exp Rheumatol*. 2023;41:67–73. doi: [10.55563/clinexprheumatol/fe4go6](https://doi.org/10.55563/clinexprheumatol/fe4go6)
22. Martín-González C, Ferrer-Moure C, Carlos Quevedo-Abeledo J, de Vera-González A, González-Delgado A, Sánchez-Martín J, González-Gay MÁ, Ferraz-Amaro I. Apolipoprotein C-III in patients with systemic lupus erythematosus. *Arthritis Res Ther*. 2022;24:104. doi: [10.1186/s13075-022-02793-y](https://doi.org/10.1186/s13075-022-02793-y)
 23. Gong T, Zhou R. ApoC3: an 'alarmin' triggering sterile inflammation. *Nat Immunol*. 2020;21:9–11. doi: [10.1038/s41590-019-0562-3](https://doi.org/10.1038/s41590-019-0562-3)
 24. Li J, Sun H, Wang Y, Liu J, Wang G. Apolipoprotein C3 is negatively associated with estrogen and mediates the protective effect of estrogen on hypertriglyceridemia in obese adults. *Lipids Health Dis*. 2023;22:29. doi: [10.1186/s12944-023-01797-0](https://doi.org/10.1186/s12944-023-01797-0)
 25. Kanter JE, Bornfeldt KE. Apolipoprotein C3 and apolipoprotein B colocalize in proximity to macrophages in atherosclerotic lesions in diabetes. *J Lipid Res*. 2021;62:100010. doi: [10.1194/jlr.ILR120001217](https://doi.org/10.1194/jlr.ILR120001217)
 26. Ramírez CM, Zhang X, Bandyopadhyay C, Rotllan N, Sugiyama MG, Aryal B, Liu X, He S, Kraehling JR, Ulrich V, et al. Caveolin-1 regulates atherogenesis by attenuating low-density lipoprotein transcytosis and vascular inflammation independently of endothelial nitric oxide synthase activation. *Circulation*. 2019;140:225–239. doi: [10.1161/CIRCULATIONAHA.118.038571](https://doi.org/10.1161/CIRCULATIONAHA.118.038571)
 27. Giammanco A, Spina R, Cefalù AB, Aversa M. APOC-III: a gatekeeper in controlling triglyceride metabolism. *Curr Atheroscler Rep*. 2023;25:67–76. doi: [10.1007/s11883-023-01080-8](https://doi.org/10.1007/s11883-023-01080-8)
 28. Bennett CF. Therapeutic antisense oligonucleotides are coming of age. *Annu Rev Med*. 2019;70:307–321. doi: [10.1146/annurev-med-041217-010829](https://doi.org/10.1146/annurev-med-041217-010829)
 29. Gaudet D, Alexander VJ, Baker BF, Brisson D, Tremblay K, Singleton W, Geary RS, Hughes SG, Viney NJ, Graham MJ, et al. Antisense inhibition of Apolipoprotein C-III in patients with hypertriglyceridemia. *N Engl J Med*. 2015;373:438–447. doi: [10.1056/NEJMoa1400283](https://doi.org/10.1056/NEJMoa1400283)
 30. Alexander VJ, Xia S, Hurh E, Hughes SG, O'Dea L, Geary RS, Witztum JL, Tsimikas S. N-acetyl galactosamine-conjugated antisense drug to apo C3 mRNA, triglycerides and atherogenic lipoprotein levels. *Eur Heart J*. 2019;40:2785–2796. doi: [10.1093/eurheartj/ehz209](https://doi.org/10.1093/eurheartj/ehz209)
 31. Gaudet D, Pall D, Watts GF, Nicholls SJ, Rosenson RS, Modesto K, San Martin J, Hellawell J, Ballantyne CM. Plozasiran (ARO-apo C3) for severe hypertriglyceridemia: the SHASTA-2 randomized clinical trial. *JAMA Cardiol*. 2024;9:620–630. doi: [10.1001/jamacardio.2024.0959](https://doi.org/10.1001/jamacardio.2024.0959)